ORIGINAL RESEARCH

Effects of Post-Resuscitation Normoxic Therapy on Oxygen-Sensitive Oxidative Stress in a Rat Model of Cardiac Arrest

Yu Okuma (iD), MD, PhD*; Lance B. Becker, MD; Kei Hayashida (iD), MD, PhD; Tomoaki Aoki (iD), MD, PhD; Kota Saeki, MEng; Mitsuaki Nishikimi, MD; Muhammad Shoaib (iD), BA; Santiago J. Miyara (iD), MD; Tai Yin, MD, PhD; Koichiro Shinozaki (iD), MD, PhD*

BACKGROUND: Cardiac arrest (CA) can induce oxidative stress after resuscitation, which causes cellular and organ damage. We hypothesized that post-resuscitation normoxic therapy would protect organs against oxidative stress and improve oxygen metabolism and survival. We tested the oxygen-sensitive reactive oxygen species from mitochondria to determine the association with hyperoxia-induced oxidative stress.

METHODS AND RESULTS: Sprague–Dawley rats were subjected to 10-minute asphyxia-induced CA with a fraction of inspired O_2 of 0.3 or 1.0 (normoxia versus hyperoxia, respectively) after resuscitation. The survival rate at 48 hours was higher in the normoxia group than in the hyperoxia group (77% versus 28%, $P<0.01$), and normoxia gave a lower neurological deficit score (359±140 versus 452±85, $P<0.05$) and wet to dry weight ratio (4.6±0.4 versus 5.6±0.5, $P<0.01$). Oxidative stress was correlated with increased oxygen levels: normoxia resulted in a significant decrease in oxidative stress across multiple organs and lower oxygen consumption resulting in normalized respiratory quotient (0.81±0.05 versus 0.58±0.03, $P<0.01$). After CA, mitochondrial reactive oxygen species increased by ≈2-fold under hyperoxia. Heme oxygenase expression was also oxygen-sensitive, but it was paradoxically low in the lung after CA. In contrast, the HMGB-1 (high mobility group box-1) protein was not oxygen-sensitive and was induced by CA.

CONCLUSIONS: Post-resuscitation normoxic therapy attenuated the oxidative stress in multiple organs and improved post-CA organ injury, oxygen metabolism, and survival. Additionally, post-CA hyperoxia increased the mitochondrial reactive oxygen species and activated the antioxidation system.

Key Words: hyperoxia ■ ischemic reperfusion injury ■ mitochondrial dysfunction ■ oxidative stress ■ oxygen consumption

Cardiac arrest (CA) is a major public health issue affecting ≈600 000 people each year in the United States.[1] New therapies to reduce the occurrence and extent of organ injury, and the resulting pathophysiology, are imperative to improve patient survival and quality of life after CA.[2,3]

In the context of reperfusion injury, hyperoxia is thought to cause cellular damage by increasing the generation of reactive oxygen species (ROS), resulting in an exacerbation of oxidative toxic stress, deterioration of mitochondrial dysfunction, and derangement of cellular metabolism.[4–6] Compelling data from clinical and preclinical trials have demonstrated benefits of post-CA normoxic therapy.[4,5,7–17]

The purpose of post-resuscitation normoxic therapy is to reduce ROS generation and consequently

CLINICAL PERSPECTIVE

What Is New?

- The results reported here indicate that cardiac arrest is associated with mitochondrial dysfunction and that the amount of mitochondrial reactive oxygen species generation could be doubled in the brain when these are exposed to hyperoxic conditions.

What Are the Clinical Implications?

- This study provides much-needed evidence of the augmentation of the O_2-sensitivity of mitochondria in the generation of reactive oxygen species after cardiac arrest.
- Mitochondrial reactive oxygen species generation during hyperoxia is therefore likely a causal factor in upregulating the oxidizing pathways.
- Our finding implies the important pathophysiology linked with post-cardiac arrest organ failure.

Nonstandard Abbreviations and Acronyms

AGE	advanced glycation end product
CA	cardiac arrest
HMGB	high mobility group box
HO	heme oxygenase
ROS	reactive oxygen species
RQ	respiratory quotient
VCO$_2$	carbon dioxide production
VO$_2$	oxygen consumption

attenuate oxidative stress after CA. Although the rationale for post-resuscitation normoxic therapy is well established,[3,7,10,11] its mechanism and specifically the role of mitochondrial ROS in post-CA pathophysiology have not been clearly elucidated. Evidence has shown that mitochondria play a crucial role as effectors and targets of ischemia/reperfusion injury such as CA.[18–21] Mitochondrial ROS generation is theoretically oxygen-sensitive[22]; indeed, decreased production of ROS by isolated mitochondria was observed when the O_2 was lowered below that of the air-saturated medium.[23] However, though it is widely accepted that CA victims are afflicted by hyperoxia-induced organ damage[12] caused by an exacerbation of oxidative stress attributable to ongoing mitochondrial dysfunction,[24] the O_2-sensitive mitochondrial ROS generation and its augmentation by CA has not been shown.

We previously reported on a system-level derangement of post-CA metabolism characterized by dissociated oxygen consumption (VO_2) and carbon dioxide production (VCO_2), resulting in a lowered respiratory

quotient (RQ). This newly found phenotype was O_2 sensitive.[25] In the present study, we use a rat cardiopulmonary resuscitation (CPR) model to test (1) whether hyperoxia-induced injury is mediated by mitochondrial ROS production and increased inflammation and (2) whether normoxic post-resuscitation therapy protects against oxidative stress in several organs and improves systematic oxygen metabolism.

METHODS

The Institutional Animal Care and Use Committees of the Feinstein Institutes for Medical Research approved this study protocol. We performed all instrumentation and surgical preparation according to our previously described protocol.[25] Details are found in Data S1. The data that support the findings of this study are available from the corresponding author upon reasonable request.

Comparing Hyperoxia and Normoxia

Sprague–Dawley male rats (n=30) were randomly assigned into 2 groups 10 minutes after CPR. Successfully resuscitated animals were given normoxic (30% oxygen, inhaled, n=15) or hyperoxic (100% oxygen, inhaled, n=15) therapy (Figure S1A). Oxygen therapy continued for up to 2 hours and monitoring for up to 48 hours, at which point neurological deficit score was taken as described previously.[26]

VO$_2$, VCO$_2$, and RQ Measurements

Using the mechanical ventilation circuit, we evaluated the system-level metabolic alteration for up to 120 minutes via VO_2, VCO_2, and RQ (RQ=VCO_2/VO_2 as previously described[25]). We added 2 major modifications to obtain VO_2 more accurately at a fraction of inspired O_2 of 1.0. First, we used a CO_2 mainstream capnometer (Nihon Kohden Corp., Tokyo, Japan) to avoid sampling (suctioning) the gas from the ventilation system. Secondly, we measured the molecular ratio of inhalation to exhalation, which was an independent measurement from the gas concentration measurements. The values were calculated and reported as standard temperature and pressure.

Immunochemical Assays of Oxidative Stress Indicators, HO-1, and HMGB-1

Carbonyl protein and 8-hydroxy-2′-deoxyguanosine levels were measured as an indicator of oxidative stress. Heme oxygenase (HO)-1 is a cytoprotective antioxidant enzyme,[27] and the HO-1 level was measured as an indicator of the activation of the antioxidant system. The HMGB-1 (high mobility group box-1) protein is an inflammatory alarmin that is released following

non-programmed cell death, but by apoptotic cells.[28] We measured HMGB-1 levels as an indicator of the activation of inflammatory pathways. These biomarkers were measured by ELISA based on the commercial protocol.

Isolation of Brain and Kidney Mitochondria and Evaluation of Mitochondrial Respiratory Function

Mitochondrial samples were collected from the sham-normoxia and CA-normoxia groups. All isolations were performed at 4°C. Brain and kidney mitochondria were isolated using a procedure modified from Kim et al.[20,29] The oxygen consumption was measured using a Strathkelvin oxygen electrode (30°C). ADP-dependent (state 3) and ADP-limited (state 4) respirations were measured in 150 μL of the mitochondrial suspension (0.5 mg/mL) using glutamate and malate as substrates.

Comparing Mitochondrial H_2O_2 Generation in Ex Vivo Normoxic and Hyperoxic Conditions

H_2O_2 generation in mitochondria isolated from brain and kidney was used as a measure of mitochondrial ROS and compared between sham-normoxia and CA-normoxia experimental groups. Two different O_2 tension settings were applied to the mitochondria of each group. Different O_2 concentrations in the medium were achieved by mixing nitrogen- and air-saturated buffers (Figure S2). H_2O_2 levels were determined using an Amplex Red hydrogen peroxide/peroxidase assay kit (Invitrogen, Carlsbad, CA, USA), as instructed by the manufacturer. The mitochondria were incubated at 0.025 mg of protein/mL at 30°C. H_2O_2 production was initiated in the mitochondria using glutamate (10 mmol/L) and malate (2.5 mmol/L) as substrates, using an established protocol[30] (Figure S3).

Wet/Dry Weight Ratio of the Lung

The right lower lobe from each animal was weighed immediately after collection and then placed into a 60°C oven to dry. After 3 days, the tissue was weighed to determine the wet-to-dry lung weight ratio (W/D).

Immunofluorescence Staining of HO-1 and HMGB-1 and Histological Lung Injury Evaluation

Double immunostaining was performed for HMGB-1 or advanced glycation end product (AGE) in combination with HO-1. Stained sections were observed under an LSM 880 confocal imaging system (Carl Zeiss, Inc., Jena, Germany) and a BZ-X800 all-in-one fluorescence microscope (Keyence, Elmwood Park, NJ, USA). We analyzed the data using the BZ-X800 analyzer software (Keyence, Elmwood Park, NJ, USA). The lung sections were also stained with hematoxylin and eosin. A blinded investigator reviewed the histopathology using a modified acute lung injury scoring system, as previously described by Kawamura et al.[31]

Statistical Analysis

Data are shown as the means and SD for continuous variables and the counts and frequencies for categorical variables. Mann-Whitney U test was used to compare 2 independent groups for continuous variables. For multi group comparisons, Kruskal–Wallis test with the Dunn-Bonferroni approach were used. Survival rates were estimated by the Kaplan–Meier method, and the Wilcoxon test was used to compare the groups. Two-tailed P values were calculated, and $P<0.05$ was considered statistically significant. SPSS 25.0 (IBM, Armonk, NY, USA), JMP 10.1 (SAS Institute, Cary, NC, USA), and GraphPad Prism 8 (GraphPad Software, San Diego, CA, USA) were used for statistical analyses.

RESULTS

Post-Resuscitation Normoxic Therapy Improved Neurological Function and Survival After CA

The normoxic therapy group demonstrated a higher survival rate (77%) at 48 hours after resuscitation compared with the hyperoxia group (28%, $P=0.010$: Figure S1B). Along with improved survival rates, the normoxic therapy group had significantly lower neurological deficit score (359±140) compared with the hyperoxia group (452±85, $P=0.026$: Figure S1C).

Post-Resuscitation Normoxic Therapy Reduced System-Level Dissociations of Oxygen Metabolism

At 120 minutes after CPR, the sham group had normal values of VO_2, VCO_2, and RQ (14.3±1.5 mL/kg per minute, 14.1±1.4 mL/kg per minute, and 0.99±0.12, respectively). At 120 minutes after CPR, the VO_2 in the CA-normoxia group was significantly lower over time (17.8±3.1 mL/kg per minute) than in the CA-hyperoxia group (31.1±5.2 mL/kg per minute, Kruskal–Wallis; $P=0.002$, pairwise $P=0.003$: Figure 1B). There were no differences in VCO_2 between the groups (Kruskal–Wallis; $P=0.080$: Figure 1C). As a result, the RQ after
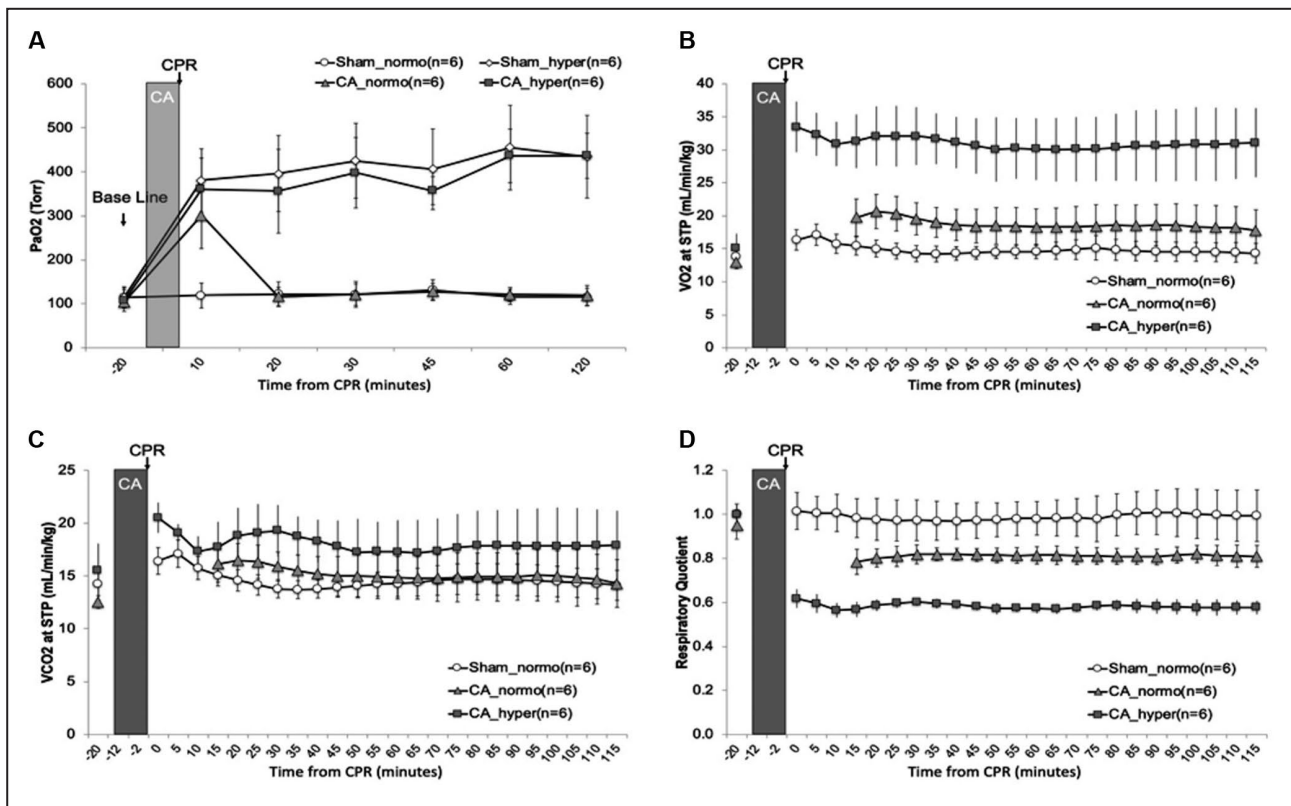
Figure 1. Post-resuscitation normoxic therapy reduced system-level dissociations of oxygen metabolism in a rat cardiopulmonary resuscitation model.

A, PaO_2 levels over time compared among the groups. There were no significant differences in the values of PaO_2 at 10 minutes between the normoxia and hyperoxia (302 ± 76 and 361 ± 71 Torr, respectively). In the normoxic therapy group, PaO_2 was successfully maintained at 120 ± 10 Torr during the initial 120 minutes after randomization. PaO_2 levels in the hyperoxia group were higher than 350 Torr at all times. Time (min) from starting CPR is depicted on the *x*-axis. **B**, VO_2 over time. Values were averaged every 5 minutes. The VO_2 in the CA-normoxia group was significantly lower over time. **C**, Carbon dioxide production over time. Values were averaged every 5 minutes. There were no differences in carbon dioxide production between the groups. **D**, Respiratory quotient over time. The respiratory quotient after CA was significantly higher in the CA-normoxia group than it was in the CA-hyperoxia group, and the value for the normoxia group improved to the generally cited normal range of 0.7 to 1.0; mean±SD, Kruskal−Wallis test with the post hoc analysis. CA indicates cardiac arrest; CPR, cardiopulmonary resuscitation; STP, standard temperature and pressure.

CA was significantly higher in the CA-normoxia group (0.81 ± 0.05) than in the CA-hyperoxia group (0.58 ± 0.03, Kruskal−Wallis; $P=0.001$, pairwise $P=0.001$: Figure 1D), and the value for the normoxia group improved to the generally cited normal range of 0.7 to 1.0.

Post-Resuscitation Normoxic Therapy Protected Organs Against Oxidative Stress

During hyperoxia, an increase in the amounts of carbonyl protein in the brain were observed in the CA group (sham-normoxia and hyperoxia, 0.15 ± 0.14 and 0.33 ± 0.05 nmol/mg protein; CA-normoxia and hyperoxia, 0.32 ± 0.23 and 0.93 ± 0.13 nmol/mg protein; Kruskal−Wallis; $P<0.001$, pairwise $P=0.396$, $P=0.005$, respectively: Figure 4A). The carbonyl protein levels were O_2-sensitive, and a similar trend was observed in the sham group. However,

hyperoxia-induced a more substantial increase in carbonyl protein levels in the CA group.

Additionally, hyperoxia induced an increase in carbonyl protein in the lung in both the sham and CA groups (sham-normoxia and hyperoxia, 0.13 ± 0.07 and 0.42 ± 0.07 nmol/mg protein; CA-normoxia and hyperoxia, 0.28 ± 0.15 and 1.00 ± 0.14 nmol/mg protein; Kruskal−Wallis; $P<0.001$, pairwise $P=0.028$, $P=0.006$, respectively: Figure 2B). Hyperoxia also increased 8-hydroxy-2′-deoxyguanosine levels in the tracheal secretion in the CA group (sham-normoxia and hyperoxia, 3.2 ± 1.5 and 5.6 ± 0.5 ng/mL; CA-normoxia and hyperoxia, 7.6 ± 1.2 and 20 ± 6 ng/mL; Kruskal−Wallis; $P<0.001$, pairwise $P=0.901$, $P=0.528$, respectively: Figure 2D). CA-induced increase in 8-hydroxy-2′-deoxyguanosine levels was greater than in the sham animals in both normoxia and hyperoxia settings ($P=0.006$ and $P=0.002$, respectively).
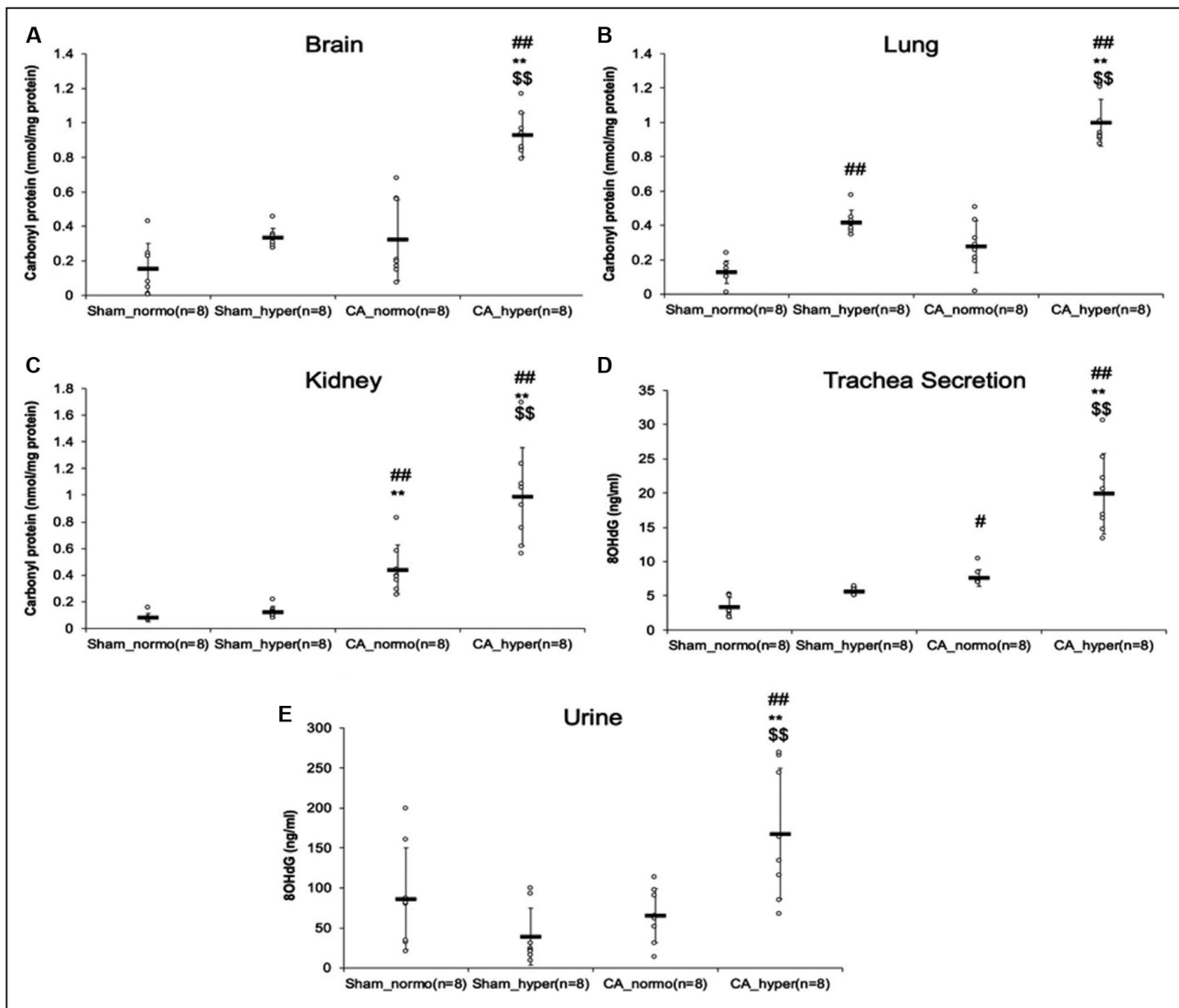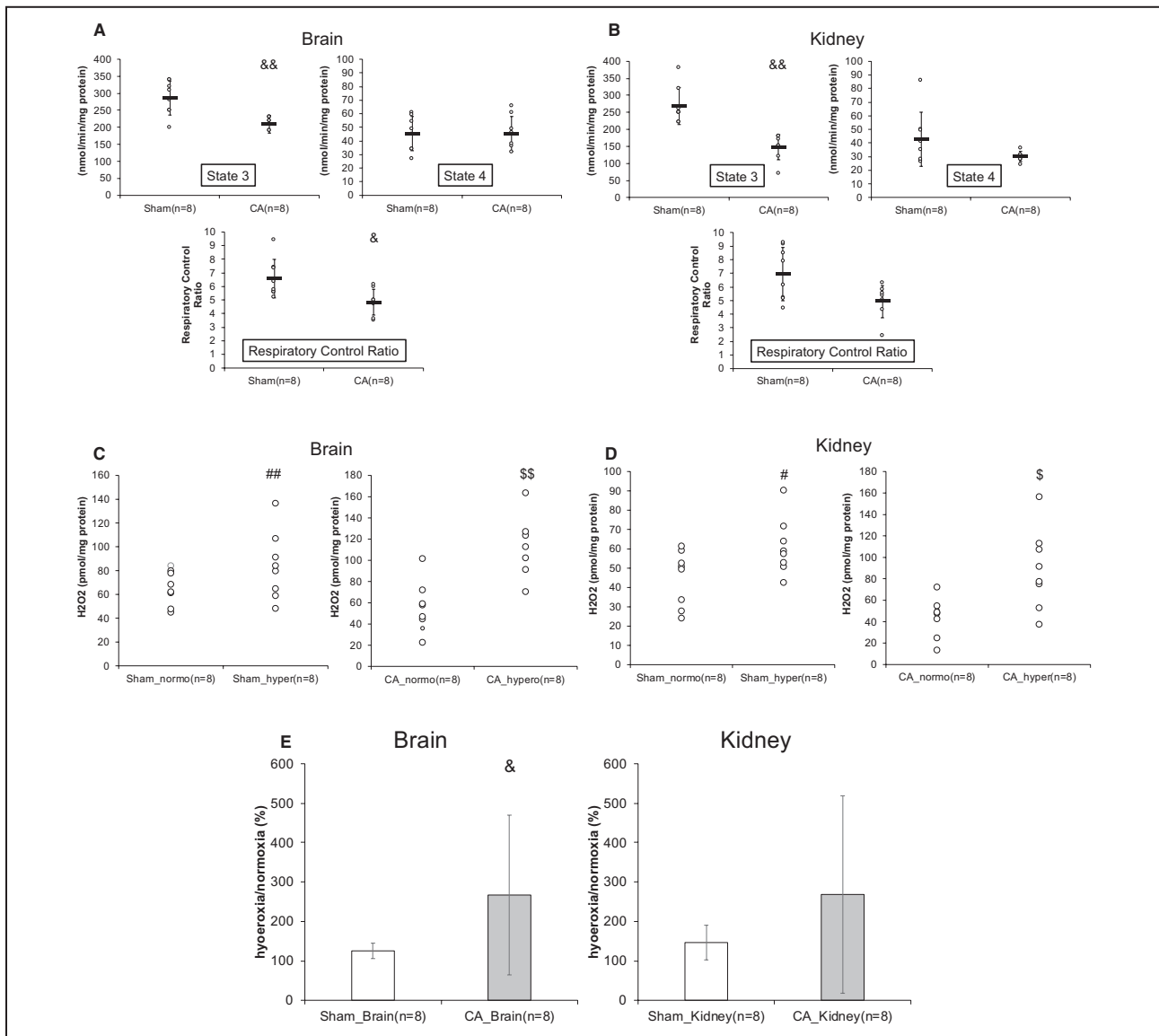
Figure 2. Post-resuscitation normoxic therapy reduced carbonyl protein levels in the organs and 8-hydroxy-2′-deoxyguanosine (8OHdG) levels in tracheal secretions and urine.
A, Carbonyl protein levels in the brain. **B**, Carbonyl protein levels in the lung. **C**, Carbonyl protein levels in the kidney. The carbonyl protein levels were O_2 dependent, and there was a trend in O_2 dependency in the sham group. However, hyperoxia-induced increases in carbonyl protein were more remarkable in the cardiac arrest (CA) group ($P<0.01$). **D**, 8OHdG levels in tracheal secretions. Hyperoxia also increased the 8OHdG levels of the tracheal secretion in the CA group. A supply of 100% oxygen via the endotracheal tube did not affect the 8OHdG levels in the tracheal secretion samples from sham animals. Consequently, O_2 dependency was only observed in the CA animals ($P<0.01$). **E**, 8OHdG levels in urine samples. A supply of 100% oxygen did not affect the 8OHdG levels in the urine samples from sham animals. Consequently, O_2 dependency was only observed in CA animals ($P<0.01$). CA indicates cardiac arrest; and 8OHdG, 8-hydroxy-2′-deoxyguanosine. ##$P<0.01$ vs sham normoxia. **$P<0.01$ vs sham hyperoxia. $$$P<0.01$ vs CA normoxia; mean±SD, Kruskal−Wallis test with the post hoc analysis.

A hyperoxia-induced increase in carbonyl protein in the kidney was also observed in the CA group (sham-normoxia and hyperoxia, 0.08±0.03 and 0.12±0.04 nmol/mg protein; CA-normoxia and hyperoxia, 0.44±0.18 and 0.99±0.37 nmol/mg protein; Kruskal−Wallis; $P<0.001$, pairwise $P=1.000$, $P=0.814$, respectively: Figure 2C). Hyperoxia also increased 8-hydroxy-2′-deoxyguanosine levels in the urine of the CA group (sham-normoxia and hyperoxia, 87±63 and 39±36 ng/mL; CA-normoxia and hyperoxia, 65±34 and 168±81 ng/mL; Kruskal−Wallis; $P=0.005$, pairwise $P=0.659$, $P=0.099$, respectively: Figure 2E).

These results support the concept that oxidative stress is O_2-sensitive overall and can be seen in multiple organs even in non-injured animals. However, there is an augmentation of oxygen-sensitivity induced by CA. Thus, post-resuscitation normoxic therapy significantly protected the animals against oxidative toxic stress.
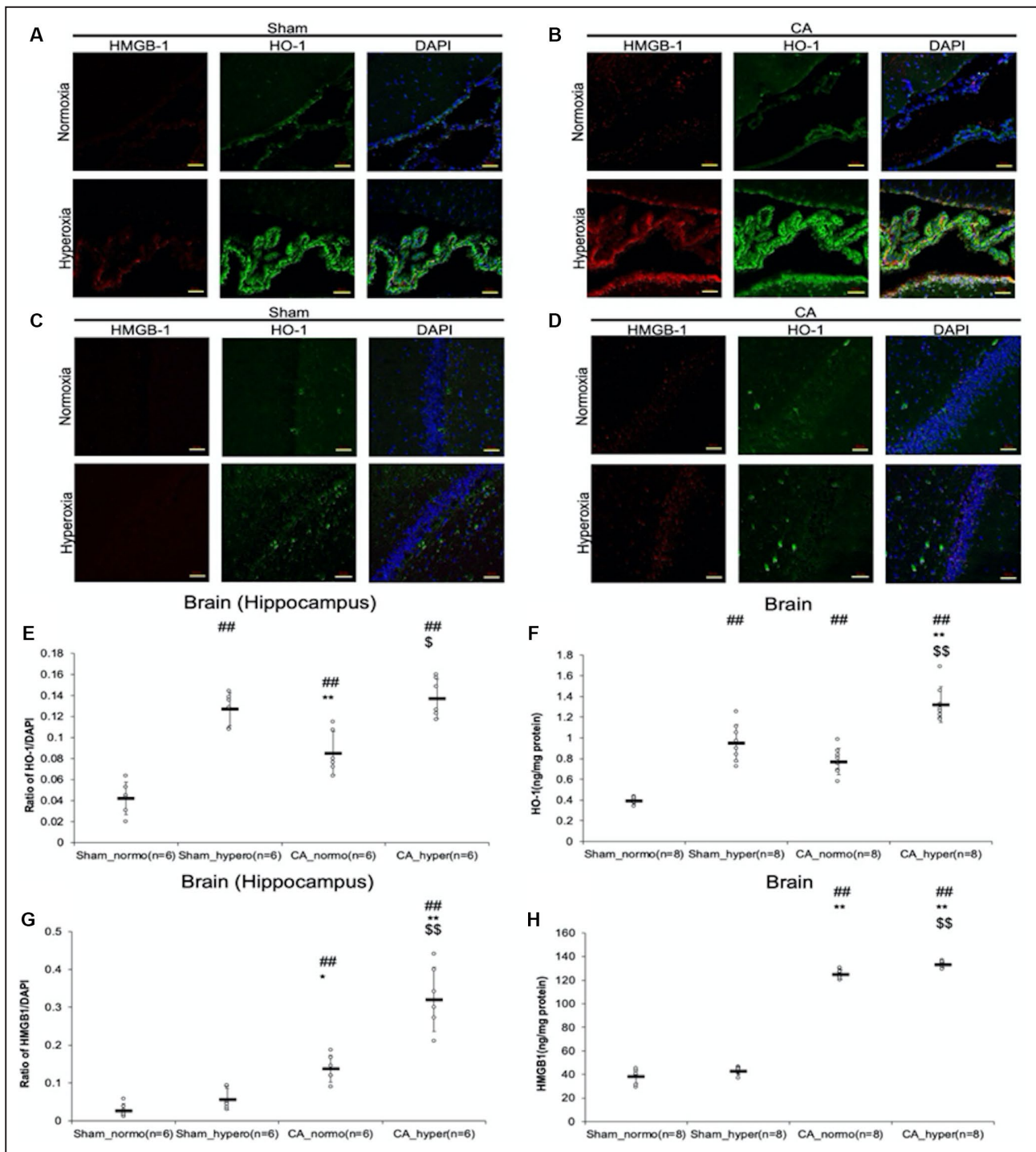
Figure 3. Cardiac arrest (CA) decreased state 3 mitochondrial respiratory activity and increased the degree of hyperoxia-induced increases in mitochondrial H_2O_2 generation.

A, Mitochondrial respiratory activity in the brain. **B**, Mitochondrial respiratory activity in the kidney. The state 3 respiration activity of the brain and the kidney mitochondria in the CA-normoxia group declined significantly compared with that of the sham-normoxia group. In contrast, the state 4 respiration activity of the brain and the kidney mitochondria did not change significantly. &&$P<0.01$ vs sham. **C**, Mitochondrial H_2O_2 generation in the brain. **D**, Mitochondrial H_2O_2 generation in the kidney. The ex vivo hyperoxic condition significantly accelerated the H_2O_2 generation of the brain and the kidney mitochondria in both the sham and CA groups. **E**, O_2 dependency of mitochondrial H_2O_2 generation compared between CA and sham animals. The brain mitochondria generated approximately twice as much H_2O_2 under hyperoxia. The kidney mitochondria also showed a similar trend, but there was no statistical significance. CA indicates cardiac arrest. #$P<0.05$, ##$P<0.01$ vs sham normoxia. $$P<0.05$, $$$P<0.01$ vs CA normoxia. &$P<0.05$ vs sham; mean±SD, Mann-Whitney U test.

Cardiac Arrest Induces Mitochondrial Respiratory Dysfunction and the Augmentation of O_2-Sensitive Mitochondrial H_2O_2 Generation
Oxidative Phosphorylation

The state 3 respiration activity of the brain and kidney mitochondria in the CA-normoxia group (209±26 and 148±37 nmol/min per mg) declined significantly compared with those of the sham-normoxia group (286±50 and 269±55 nmol/min per mg; $P=0.003$, $P=<0.001$, respectively: Figure 3A and 3B). In contrast, the state 4 respiration activity of the brain and kidney mitochondria did not change. As a result, the respiratory control ratio showed an altered trend after CA in both tissues.

Figure 4. Hyperoxia increased heme oxygenase-1 (HO-1) levels and cardiac arrest (CA) increased both HO-1 and HMGB-1 (high mobility group box 1) levels in the brain.

A, Immunohistochemistry studies of the choroid plexus and subependymal cell layer areas in sham animals. **B**, The choroid plexus and subependymal cell layer areas in CA animals. **C**, The hippocampus area in sham animals. **D**, The hippocampus area in CA animals. Images were captured in a low power field and the yellow bars represent a scale of 50 µm. **E**, Ratio of HO-1 to 4′,6-diamidino-2-phenylindole fluorescent stain in the hippocampus area. **F**, HO-1 levels in the brain by ELISA. Hyperoxia induced an increase in HO-1 expression in both the sham and CA groups. Based on a comparison between the sham and CA animals at normoxia ($P<0.01$), CA also seemed to induce HO-1 expression. **G**, Ratio of HMGB-1 to 4′,6-diamidino-2-phenylindole fluorescent stain in the hippocampus area. **H**, HMGB-1 levels in the brain by ELISA. CA increased the HMGB-1 levels. There may be a correlation between O_2 dependency and HMGB-1 levels, but this was only observed post-CA. [#]$P<0.05$, [##]$P<0.01$ vs sham normoxia. CA indicates cardiac arrest; HMGB-1, high mobility group box 1; HO-1, heme oxygenase 1; DAPI is a 4′,6-diamidino-2-phenylindole fluorescent stain. [*]$P<0.05$, [**]$P<0.01$ vs sham hyperoxia. [$]$P<0.05$, [$$]$P<0.01$ vs CA normoxia; mean±SD, Kruskal–Wallis test with the post hoc analysis.

H₂O₂ Generation in Mitochondria

Ex vivo hyperoxia significantly accelerated H_2O_2 generation in brain mitochondria in both the sham and CA groups (sham-normoxia and hyperoxia, 66±13 and 84±29 pmol/mg protein; CA-normoxia and hyperoxia, 55±26 and 115±23 pmol/mg protein; Kruskal−Wallis; $P=0.002$, pairwise $P=1.000$, $P=0.001$, respectively: Figure 3C). A similar trend was also observed in kidney mitochondria (sham-normoxia and hyperoxia, 45±15 and 61±16 pmol/mg protein; CA-normoxia and hyperoxia, 44±14 and 89±39 pmol/mg protein; Kruskal−Wallis; $P=0.009$, pairwise $P=0.733$, $P=0.020$, respectively: Figure 3D).

The effect of ex vivo hyperoxia on mitochondrial H_2O_2 generation was calculated for each mitochondrial sample, and the numbers were averaged and compared between the groups. The brain mitochondria generated approximately twice as much H_2O_2 in the hyperoxic condition (sham and CA, 125±20% and 267±203%; $P=0.036$, respectively: Figure 3E). The kidney mitochondria also showed a similar trend, but there was no statistical significance (sham and CA, 146±43% and 268±250%; $P=0.279$, respectively: Figure 3E). These results support the augmentation of O_2-sensitive mitochondrial H_2O_2 generation after CA. This result might be attributed to the mitochondrial dysfunction observed in the CA rat model.

Hyperoxia Increased HO-1 Levels and Cardiac Arrest Increased Both HO-1 and HMGB-1 Levels in the Brain

Immunohistochemical studies of the brain revealed an O_2-sensitive increase in HO-1 expression (Figure 4A through 4D).The ratio of HO-1 positive to 4′,6-diamidino-2-phenylindole fluorescent stain positive areas (Figure 4E) showed a similar trend with the quantitative measurement of HO-1 levels by ELISA (sham-normoxia and hyperoxia, 0.39±0.03, 0.95±0.18 ng/mg protein; CA-normoxia and hyperoxia, 0.77±0.13 and 1.32±0.17 ng/mg protein, Kruskal−Wallis; $P<0.001$, pairwise $P=0.010$, $P=0.017$, respectively: Figure 4F).

Immunohistochemical studies of the brain also revealed a CA-induced increase in HMGB-1 (Figure 4A through 4D). The ratio of HMGB-1 positive to 4′,6-diamidino-2-phenylindole fluorescent stain-positive areas (Figure 4G) showed a similar trend with the quantitative measurement of HMGB-1 levels (sham-normoxia and hyperoxia, 38.1±5.5 and 42.8±3.1 ng/mg protein; CA-normoxia and hyperoxia, 125±4 and 133±2 ng/mg protein, Kruskal−Wallis; $P<0.001$, pairwise $P=1.000$, $P=0.659$, respectively: Figure 4H). The O_2-sensitive augmentation was only observed post-CA.

Cardiac Arrest was Associated With Hyperoxic Lung Injury

The lung W/D ratio revealed that hyperoxia increased lung edema after CA (sham-normoxia and hyperoxia, 4.4±0.6 and 4.7±0.2; CA-normoxia and hyperoxia, 4.6±0.4 and 5.6±0.5, Kruskal−Wallis; $P=0.006$, pairwise $P=1.000$, $P=0.033$, respectively: Figure S4A). The lung injury score histologically similarly exhibited increased the degree of lung injury at 120 minutes after CPR because of hyperoxia (sham-normoxia and hyperoxia, 2.7±2.3 and 2.3±1.0; CA-normoxia and hyperoxia, 4.3±2.9 and 14±2; Kruskal−Wallis; $P=0.002$, pairwise $P=1.000$, $P=0.157$, respectively: Figure S4B and S4C). These results support the idea that hyperoxia induces lung injury, which is more substantial post-CA.
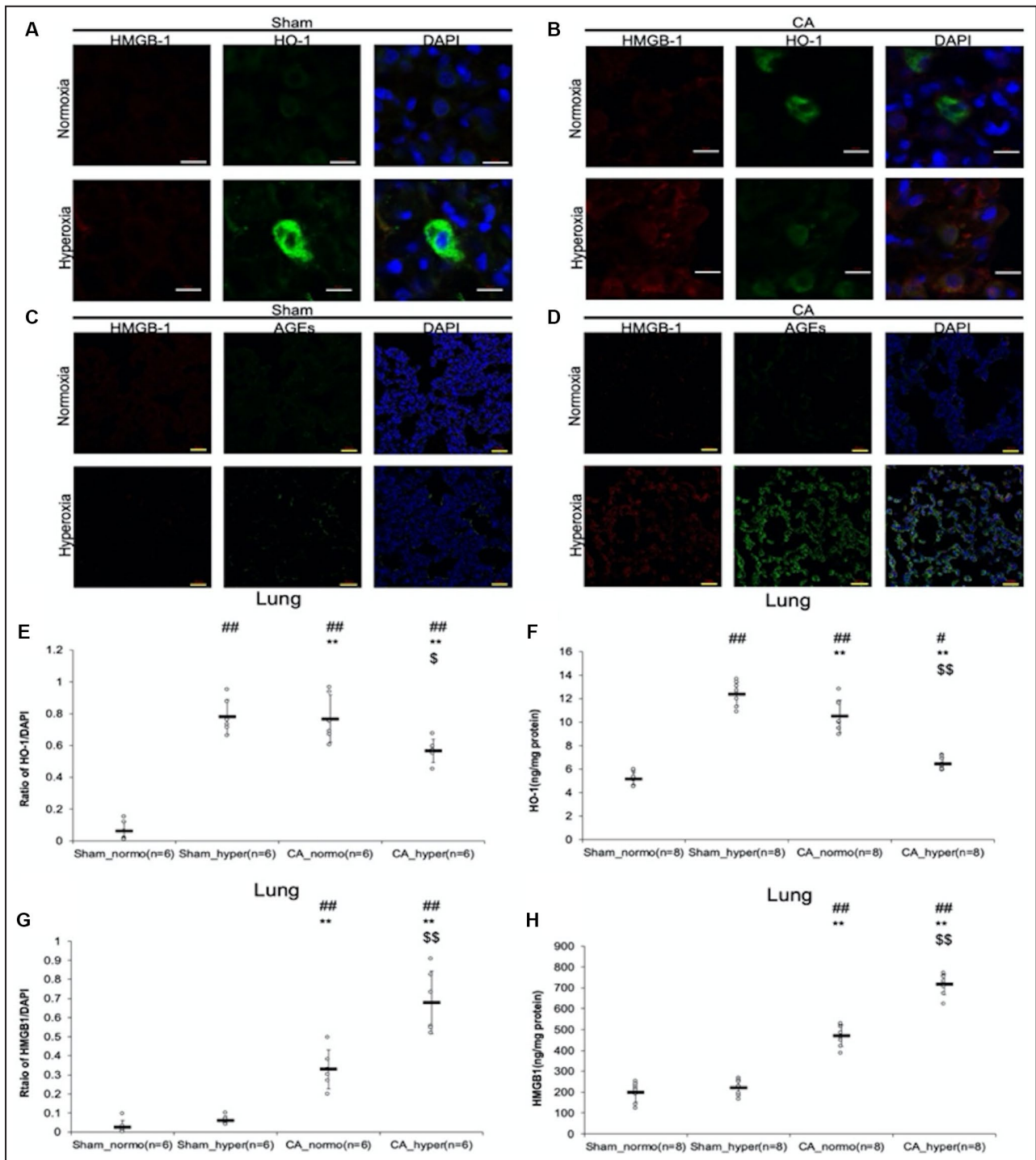
Hyperoxia Increased HO-1 Levels and Cardiac Arrest Increased Both HO-1 and HMGB-1 Levels in the Lung

Immunohistochemical studies of the lung revealed an O_2-sensitive increase in HO-1 expression in the sham animals (Figure 5A through 5D). However, this increase was suppressed by hyperoxia after CA. The ratio of HO-1-positive to 4′,6-diamidino-2-phenylindole fluorescent stain-positive (Figure 5E) areas showed that hyperoxia increased HO-1 in the sham group but not in the CA group, and quantitative ELISA showed a similar trend to the immunohistochemistry results (sham-normoxia and hyperoxia, 5.2±0.5 and 12.4±1.0 ng/mg protein; CA-normoxia and hyperoxia, 10.5±1.4 and 6.5±0.5 ng/mg protein; Kruskal−Wallis; $P<0.001$, pairwise $P<0.01$, $P=0.274$, respectively: Figure 5F).

Immunohistochemical studies also revealed an increase in HMGB-1 and AGE in the lung after CA (Figure 5A through 5D). Quantitative measurement of HMGB-1 by ELISA (Figure 5G) showed a trend similar to the immunohistochemistry results (sham-normoxia and hyperoxia, 199±46, 221±36 ng/mg protein; CA-normoxia and hyperoxia, 471±51 and 716±49 ng/mg protein; Kruskal−Wallis; $P<0.001$, pairwise $P=1.000$, $P=0.528$, respectively: Figure 5H). These results suggest that HO-1 expression in the lung is O_2-sensitive, but there may also be a paradoxical suppression of HO-1 expression post-CA during hyperoxia. CA increased HMGB-1 levels in the lung. Given the immunohistochemical finding of AGE expression in conjunction with an increase in HMGB-1, our results suggest that the inflammatory HMGB-1 pathway may be activated post-CA.

DISCUSSION

Our data demonstrate that oxidative stress is O_2-sensitive overall and occurs in multiple organs, but the increase in oxidative stress is more notable after CA. The pathophysiological response to elevated

Figure 5. Hyperoxia increased heme oxygenase-1 (HO-1) levels and cardiac arrest (CA) increased both HO-1 and HMGB-1 levels in the lung.

A, Immunohistochemistry studies of the lung in sham animals. **B**, Immunohistochemistry studies in the CA animals. Images are shown as high-power field and the white bars represent a scale of 10 μm. **C**, Immunohistochemical studies in the sham animals. **D**, Immunohistochemical studies in the CA animals. Immunohistochemical studies of the lung indicated an increase in AGE expression, especially in the CA-hyperoxia group. Images are shown as low-power field and the yellow bars represent a scale of 50 μm. **E**, Ratio of HO-1 to 4′,6-diamidino-2-phenylindole fluorescent stain in the Lung. **F**, HO-1 levels in the lung by ELISA. Hyperoxia increased the HO-1 in the sham group but not in the CA group. There was an increase and suppression of HO-1 by the hyperoxia after CA. **G**, Ratio of HMGB-1 to 4′,6-diamidino-2-phenylindole fluorescent in the lung. **H**, HMGB-1 Levels in the lung by ELISA. CA but not hyperoxia increased the HMGB-1 levels in the lung. There might be a correlation between O_2 dependency and HMGB-1 levels, but it was only observed post-CA. AGEs indicates advanced glycation end products; CA, cardiac arrest; DAPI, 4′,6-diamidino-2-phenylindole fluorescent stain; HMGB-1, high mobility group box 1; and HO-1, heme oxygenase 1. [#]$P<0.01$, [##]$P<0.05$ vs sham normoxia. [**]$P<0.01$ vs sham hyperoxia. [$]$P<0.05$, [$$]$P<0.01$ vs CA normoxia; mean±SD, Kruskal–Wallis test with the post hoc analysis.

supplemental O_2 varied between post-CA animals and normal animals because of the oxidative stress. It can be inferred that an increase in oxidants (harmful pathways) and/or down-regulation of antioxidant enzymes (protective pathways) may occur after resuscitation with hyperoxia. The post-resuscitation normoxic therapy regimen significantly protected the animals against oxidative stress and further improved their survival after CA. The results reported here indicate that CA is associated with mitochondrial dysfunction and that the amount of mitochondrial H_2O_2 generation could be doubled in the brain and kidney when these are exposed to hyperoxic conditions. Thus, this study provides much-needed evidence of the augmentation of the O_2-sensitivity of mitochondria in the generation of ROS after CA. Mitochondrial ROS generation during hyperoxia is therefore likely a causal factor in upregulating the oxidizing pathways.

Previously, exciting data from our laboratory revealed new information about post-resuscitation metabolic phenotypes: we showed a system-level derangement of metabolism characterized by the O_2-sensitive dissociation of oxygen consumption and carbon dioxide production, resulting in a lowered RQ.[25] Studies have shown that VO_2 is not dependent on O_2 levels in healthy animals and humans.[32,33] This finding is consistent with our biochemical understanding of mitochondrial respiration, which suggests that the electron transport chain is limited by nicotinamide adenine dinucleotide.[34,35] The relevance of this to our findings is the prolonged production of ROS within the electron transport chain enzymes. Under normal electron transfer, 4 electrons are required to reduce molecular oxygen to 2 water molecules. However, the creation of superoxide requires a single electron to reduce molecular oxygen to a single molecule of superoxide,[36] in which there is a shift in stoichiometry from normal oxygen usage to a requirement for more oxygen.

Heme oxygenase (HO-1) is a rate-limiting enzyme that catalyzes the oxidation of heme to biologically active molecules: iron, a gene regulator; biliverdin, an antioxidant; and carbon monoxide, a heme ligand.[37] HO-1 expression can confer cytoprotection in many lung[38] and vascular disease models.[39,40] In line with the findings of others,[37] there was an increase in HO-1 expression by hyperoxia in our study, suggesting that oxidative stress might upregulate the cytoprotective pathways within the enzymatic antioxidant role of HO-1. In addition, the HO-1 levels were high post-CA, reflecting the demands of activating protective pathways because of the ongoing post-CA pathophysiology.[41] In this scenario, hyperoxia seems to accelerate the expression of HO-1 because of the exacerbated oxidative stress after CA. However, the lung with hyperoxia showed a paradoxically low expression of HO-1, which was observed in conjunction with an increase in the inflammatory HMGB-1 and, subsequently, the receptor for AGE (RAGE) pathway. The cross-reaction between HO-1 and the HMGB-RAGE pathway regulated by peroxisome proliferator-activated receptors was suggested in a previous report using acute lung injury models.[42] Our immunohistochemical study revealed expression of AGE ligands, which contribute to a variety of microvascular and macrovascular complications by binding to RAGE.[43,44] Our results suggest that the HMGB-1/RAGE pathway was activated in the lung, particularly when the tissues were exposed to high supplemental oxygen after CA/reperfusion, and this overexpression of the inflammatory pathway may account for the paradoxical suppression of HO-1 during hyperoxia after CA. Other possible explanations for the difference in HO-1 expression in the lungs compared with other organs may be differences in the time course of organ responses. It is plausible that other organs may have suppressed HO-1 levels in later, unobserved periods post-resuscitation, but the lungs showed it much earlier and within the timeframe we observed.

This study is subject to several limitations. First, the use of a rat model to study post-CA metabolism has inherent limitations in representing human disease.[45] Secondly, our study does not distinguish the contribution of mitochondrial ROS generation from other sources of ROS, and there are multiple non-mitochondrial enzymes associated with ROS generation, such as Nicotinamide adenine dinucleotide phosphate oxidase, xanthine oxidase, and monoamine oxidase.[24] These enzymes are possible contributors to the oxidative stress that we observed in the CA animals, and these reactions are theoretically O_2-sensitive. However, our study was not designed to test for non-mitochondrial enzymes. Further investigation may focus on non-mitochondrial ROS generation and may warrant a systematic approach to evaluate the contribution of mitochondrial function to the overall generation of ROS. Thirdly, the use of isolated mitochondria is valuable for studying their contribution in oxygen-mediated ROS generation post-CA but does sacrifice some physiological context of the host tissues, necessitating a more tissue-based or in vivo approach. Finally, our study was not designed to reveal cause of death in our asphyxia-CA rat model. In nature, CA is defined as a sudden cessation of blood flow and, when the heart successfully regains the circulation, the body suffers from ischemia/reperfusion injury in multiple organ systems, and neurological function is generally the most affected.[46,47] CA may or may not be attributed to a cardiac etiology, although cardiac origin is the most prevalent in humans.[48–50] Our study protocol

of 10 minutes asphyxia may not be severe enough to affect heart function, despite the damage observed in other organs. No differences or pattern alterations were observed in Mean arterial pressure, heart rate, or blood lactate levels (representing systemic circulatory dysfunction) between the hyperoxia and normoxia groups (Figure S5A through S5C). Hyperoxia-induced augmentation of oxidative stress may worsen neurological function; however, we did not observe any augmentation in cardiac or circulatory function in the early period. Moreover, in our experimental animal model, we did not identify an increase of oxidative stress in the heart (Figure S6). Our data do not directly point to a cause of death of our animal model, but previous studies that investigated outcomes in a rat model of asphyxia-CA showed pathological and functional deficits in neurons after resuscitation,[26] and this neuronal damage may be worsened by hyperoxia.[4,5,7–17] Therefore, it is plausible that the cause of death of our asphyxia-CA model is linked to devastating neurological deficits rather than the circulatory function, once the animal has regained spontaneous circulation. However, our experimental setting did not have continuous Electroencephalography or video monitoring to allow us to assess this. Future work will focus on the cause of death by closely monitoring neurological function.

CONCLUSIONS

Our post-resuscitation normoxic therapy reduced oxidative stress in multiple organs and improved organ damage, oxygen metabolism, and survival after CA. The mitochondrial ROS generation was O_2-sensitive, and mitochondrial generation of ROS was increased after CA. HO-1 expression was also O_2-sensitive. However, a paradoxical suppression of HO-1 was observed in the lung with a concomitant upregulation of HMGB-1.

ARTICLE INFORMATION

Affiliations

From The Feinstein Institutes for Medical Research, Northwell, Manhasset, NY (Y.O., L.B.B., K.H., T.A., K.S., M.N., M.S., S.J.M., T.Y., K.S.); Department of Emergency Medicine, Donald and Barbara Zucker School of Medicine at Hofstra/Northwell, Hempstead, NY (L.B.B., K.S.); Nihon Kohden Innovation Center, Cambridge, MA (K.S.); and Elmezzi Graduate School of Molecular Medicine, Manhasset, NY (S.J.M.).

Acknowledgments

Sources of Funding

Disclosures

Supplementary Material

Data S1
Figures S1–S6
References 51–54

REFERENCES

1. Becker LB, Aufderheide TP, Graham R. Strategies to improve survival from cardiac arrest: a report from the institute of medicine. *JAMA*. 2015;314:223–224.
2. Roger VL, Go AS, Lloyd-Jones DM, Adams RJ, Berry JD, Brown TM, Carnethon MR, Dai S, de Simone G, Ford ES, et al. Heart disease and stroke statistics–2011 update: a report from the American Heart Association. *Circulation*. 2011;123:e18–e209.
3. Balan IS, Fiskum G, Hazelton J, Cotto-Cumba C, Rosenthal RE. Oximetry-guided reoxygenation improves neurological outcome after experimental cardiac arrest. *Stroke*. 2006;37:3008–3013.
4. Pilcher J, Weatherall M, Shirtcliffe P, Bellomo R, Young P, Beasley R. The effect of hyperoxia following cardiac arrest—a systematic review and meta-analysis of animal trials. *Resuscitation*. 2012;83:417–422.
5. Vereczki V, Martin E, Rosenthal RE, Hof PR, Hoffman GE, Fiskum G. Normoxic resuscitation after cardiac arrest protects against hippocampal oxidative stress, metabolic dysfunction, and neuronal death. *J Cereb Blood Flow Metab*. 2006;26:821–835.
6. Chouchani ET, Pell VR, Gaude E, Aksentijevic D, Sundier SY, Robb EL, Logan A, Nadtochiy SM, Ord EN, Smith AC, et al. Ischaemic accumulation of succinate controls reperfusion injury through mitochondrial ROS. *Nature*. 2014;515:431–435.
7. Kilgannon JH, Jones AE, Shapiro NI, Angelos MG, Milcarek B, Hunter K, Parrillo JE, Trzeciak S. Association between arterial hyperoxia following resuscitation from cardiac arrest and in-hospital mortality. *JAMA*. 2010;303:2165–2171.
8. Bellomo R, Bailey M, Eastwood GM, Nichol A, Pilcher D, Hart GK, Reade MC, Egi M, Cooper DJ. Arterial hyperoxia and in-hospital mortality after resuscitation from cardiac arrest. *Crit Care*. 2011;15:R90.
9. Helmerhorst HJ, Roos-Blom MJ, van Westerloo DJ, Abu-Hanna A, de Keizer NF, de Jonge E. Associations of arterial carbon dioxide and arterial oxygen concentrations with hospital mortality after resuscitation from cardiac arrest. *Crit Care*. 2015;19:348.
10. Vaahersalo J, Bendel S, Reinikainen M, Kurola J, Tiainen M, Raj R, Pettila V, Varpula T, Skrifvars MB. Arterial blood gas tensions after resuscitation from out-of-hospital cardiac arrest: associations with long-term neurologic outcome. *Crit Care Med*. 2014;42:1463–1470.
11. Roberts BW, Kilgannon JH, Hunter BR, Puskarich MA, Pierce L, Donnino M, Leary M, Kline JA, Jones AE, Shapiro NI, et al. Association between early hyperoxia exposure after resuscitation from cardiac arrest and neurological disability: prospective multicenter protocol-directed cohort study. *Circulation*. 2018;137:2114–2124.
12. Wang CH, Chang WT, Huang CH, Tsai MS, Yu PH, Wang AY, Chen NC, Chen WJ. The effect of hyperoxia on survival following adult cardiac arrest: a systematic review and meta-analysis of observational studies. *Resuscitation*. 2014;85:1142–1148.

13. Liu Y, Rosenthal RE, Haywood Y, Miljkovic-Lolic M, Vanderhoek JY, Fiskum G. Normoxic ventilation after cardiac arrest reduces oxidation of brain lipids and improves neurological outcome. *Stroke*. 1998;29:1679–1686.

14. Richards EM, Fiskum G, Rosenthal RE, Hopkins I, McKenna MC. Hyperoxic reperfusion after global ischemia decreases hippocampal energy metabolism. *Stroke*. 2007;38:1578–1584.

15. Brucken A, Kaab AB, Kottmann K, Rossaint R, Nolte KW, Weis J, Fries M. Reducing the duration of 100% oxygen ventilation in the early reperfusion period after cardiopulmonary resuscitation decreases striatal brain damage. *Resuscitation*. 2010;81:1698–1703.

16. Hazelton JL, Balan I, Elmer GI, Kristian T, Rosenthal RE, Krause G, Sanderson TH, Fiskum G. Hyperoxic reperfusion after global cerebral ischemia promotes inflammation and long-term hippocampal neuronal death. *J Neurotrauma*. 2010;27:753–762.

17. Danilov CA, Fiskum G. Hyperoxia promotes astrocyte cell death after oxygen and glucose deprivation. *Glia*. 2008;56:801–808.

18. Kilbaugh TJ, Sutton RM, Karlsson M, Hansson MJ, Naim MY, Morgan RW, Bratinov G, Lampe JW, Nadkarni VM, Becker LB, et al. Persistently altered brain mitochondrial bioenergetics after apparently successful resuscitation from cardiac Arrest. *J Am Heart Assoc*. 2015;4:e002232. DOI: 10.1161/JAHA.115.002232.

19. Ayoub IM, Radhakrishnan J, Gazmuri RJ. Targeting mitochondria for resuscitation from cardiac arrest. *Crit Care Med*. 2008;36:S440–446.

20. Kim J, Perales Villarroel JP, Zhang W, Yin T, Shinozaki K, Hong A, Lampe JW, Becker LB. The responses of tissues from the brain, heart, kidney, and liver to resuscitation following prolonged cardiac arrest by examining mitochondrial respiration in rats. *Oxid Med Cell Longev*. 2016;2016:7463407.

21. Han F, Da T, Riobo NA, Becker LB. Early mitochondrial dysfunction in electron transfer activity and reactive oxygen species generation after cardiac arrest. *Crit Care Med*. 2008;36:S447–S453. DOI: 10.1097/CCM.0b013e31818a8a51.

22. Murphy MP. How mitochondria produce reactive oxygen species. *Biochem J*. 2009;417:1–13. DOI: 10.1042/BJ20081386.

23. Hoffman DL, Salter JD, Brookes PS. Response of mitochondrial reactive oxygen species generation to steady-state oxygen tension: implications for hypoxic cell signaling. *Am J Physiol Heart Circ Physiol*. 2007;292:H101–H108. DOI: 10.1152/ajpheart.00699.2006.

24. Patil KD, Halperin HR, Becker LB. Cardiac arrest: resuscitation and reperfusion. *Circ Res*. 2015;116:2041–2049. DOI: 10.1161/CIRCRESAHA.116.304495.

25. Shinozaki K, Becker LB, Saeki K, Kim J, Yin T, Da T, Lampe JW. Dissociated oxygen consumption and carbon dioxide production in the post-cardiac arrest rat: a novel metabolic phenotype. *J Am Heart Assoc*. 2018;7:e007721. DOI: 10.1161/JAHA.117.007721.

26. Katz L, Ebmeyer U, Safar P, Radovsky A, Neumar R. Outcome model of asphyxial cardiac arrest in rats. *J Cereb Blood Flow Metab*. 1995;15:1032–1039. DOI: 10.1038/jcbfm.1995.129.

27. Morse D, Choi AM. Heme oxygenase-1: from bench to bedside. *Am J Respir Crit Care Med*. 2005;172:660–670. DOI: 10.1164/rccm.200404-465SO.

28. Bianchi ME. DAMPs, PAMPs and alarmins: all we need to know about danger. *J Leukoc Biol*. 2007;81:1–5. DOI: 10.1189/jlb.0306164.

29. Scholte HR, Yu Y, Ross JD, Oosterkamp II, Boonman AM, Busch HF. Rapid isolation of muscle and heart mitochondria, the lability of oxidative phosphorylation and attempts to stabilize the process in vitro by taurine, carnitine and other compounds. *Mol Cell Biochem*. 1997;174:61–66.

30. Chen Q, Vazquez EJ, Moghaddas S, Hoppel CL, Lesnefsky EJ. Production of reactive oxygen species by mitochondria: central role of complex III. *J Biol Chem*. 2003;278:36027–36031. DOI: 10.1074/jbc.M304884200.

31. Kawamura T, Huang CS, Peng X, Masutani K, Shigemura N, Billiar TR, Okumura M, Toyoda Y, Nakao A. The effect of donor treatment with hydrogen on lung allograft function in rats. *Surgery*. 2011;150:240–249.

32. Lauscher P, Lauscher S, Kertscho H, Habler O, Meier J. Hyperoxia reversibly alters oxygen consumption and metabolism. *ScientificWorldJournal*. 2012;2012:410321.

33. Lodato RF. Decreased O_2 consumption and cardiac output during normobaric hyperoxia in conscious dogs. *J Appl Physiol (1985)*. 1989;67:1551–1559.

34. Stein LR, Imai S. The dynamic regulation of NAD metabolism in mitochondria. *Trends Endocrinol Metab*. 2012;23:420–428.

35. Lane N. *Power, Sex, Suicide, Mitochondria and the Meaning of Life*. New York: Oxford University Press Inc.; 2005.

36. Wagner BA, Venkataraman S, Buettner GR. The rate of oxygen utilization by cells. *Free Radic Biol Med*. 2011;51:700–712.

37. Maines MD. The heme oxygenase system: a regulator of second messenger gases. *Annu Rev Pharmacol Toxicol*. 1997;37:517–554.

38. Morse D, Lin L, Choi AM, Ryter SW. Heme oxygenase-1, a critical arbitrator of cell death pathways in lung injury and disease. *Free Radic Biol Med*. 2009;47:1–12.

39. Choi AM, Alam J. Heme oxygenase-1: function, regulation, and implication of a novel stress-inducible protein in oxidant-induced lung injury. *Am J Respir Cell Mol Biol*. 1996;15:9–19.

40. Duckers HJ, Boehm M, True AL, Yet SF, San H, Park JL, Clinton Webb R, Lee ME, Nabel GJ, Nabel EG. Heme oxygenase-1 protects against vascular constriction and proliferation. *Nat Med*. 2001;7:693–698.

41. Xia D, Zhang H. Effects of mild hypothermia on expression of NF-E2-related factor 2 and heme-oxygenase-1 in cerebral cortex and hippocampus after cardiopulmonary resuscitation in rats. *Iran J Basic Med Sci*. 2017;20:1002–1008.

42. Wang G, Han D, Zhang Y, Xie X, Wu Y, Li S, Li M. A novel hypothesis: up-regulation of HO-1 by activation of PPARgamma inhibits HMGB1-RAGE signaling pathway and ameliorates the development of ALI/ARDS. *J Thorac Dis*. 2013;5:706–710.

43. Goldin A, Beckman JA, Schmidt AM, Creager MA. Advanced glycation end products: sparking the development of diabetic vascular injury. *Circulation*. 2006;114:597–605.

44. Byun K, Yoo Y, Son M, Lee J, Jeong GB, Park YM, Salekdeh GH, Lee B. Advanced glycation end-products produced systemically and by macrophages: a common contributor to inflammation and degenerative diseases. *Pharmacol Ther*. 2017;177:44–55.

45. Seok J, Warren HS, Cuenca AG, Mindrinos MN, Baker HV, Xu W, Richards DR, McDonald-Smith GP, Gao H, Hennessy L, et al. Genomic responses in mouse models poorly mimic human inflammatory diseases. *Proc Natl Acad Sci USA*. 2013;110:3507–3512.

46. Madl C, Holzer M. Brain function after resuscitation from cardiac arrest. *Curr Opin Crit Care*. 2004;10:213–217.

47. Morrison LJ, Visentin LM, Kiss A, Theriault R, Eby D, Vermeulen M, Sherbino J, Verbeek PR. Validation of a rule for termination of resuscitation in out-of-hospital cardiac arrest. *N Engl J Med*. 2006;355:478–487.

48. Neumar RW, Nolan JP, Adrie C, Aibiki M, Berg RA, Bottiger BW, Callaway C, Clark RS, Geocadin RG, Jauch EC, et al. Post-cardiac arrest syndrome: epidemiology, pathophysiology, treatment, and prognostication: a consensus statement from the International Liaison Committee on Resuscitation (American Heart Association, Australian and New Zealand Council on Resuscitation, European Resuscitation Council, Heart and Stroke Foundation of Canada, InterAmerican Heart Foundation, Resuscitation Council of Asia, and the Resuscitation Council of Southern Africa); the American Heart Association Emergency Cardiovascular Care Committee; the Council on Cardiovascular Surgery and Anesthesia; the Council on Cardiopulmonary, Perioperative, and Critical Care; the Council on Clinical Cardiology; and the Stroke Council. *Circulation*. 2008;118:2452–2483.

49. Kitamura T, Iwami T, Kawamura T, Nagao K, Tanaka H, Hiraide A. Nationwide public-access defibrillation in Japan. *N Engl J Med*. 2010;362:994–1004.

50. Cobb LA, Fahrenbruch CE, Olsufka M, Copass MK. Changing incidence of out-of-hospital ventricular fibrillation, 1980–2000. *JAMA*. 2002;288:3008–3013.

51. Okuma YU, Liu K, Wake H, Liu R, Nishimura Y, Hui Z, Teshigawara K, Haruma J, Yamamoto Y, Yamamoto H, et al. Glycyrrhizin inhibits traumatic brain injury by reducing HMGB1-RAGE interaction. *Neuropharmacology*. 2014;85:18–26. DOI: 10.1016/j.neuropharm.2014.05.007.

52. Gayeski TE, Honig CR. Intracellular PO2 in individual cardiac myocytes in dogs, cats, rabbits, ferrets, and rats. *Am J Physiol*. 1991;260:H522–H531. DOI: 10.1152/ajpheart.1991.260.2.H522.

53. Ubbink R, Bettink MAW, Janse R, Harms FA, Johannes T, Münker FM, Mik EG. A monitor for Cellular Oxygen METabolism (COMET): monitoring tissue oxygenation at the mitochondrial level. *J Clin Monit Comput*. 2017;31:1143–1150. DOI: 10.1007/s10877-016-9966-x.

54. Mai N, Miller-Rhodes K, Knowlden S, Halterman MW. The post-cardiac arrest syndrome: a case for lung-brain coupling and opportunities for neuroprotection. *J Cereb Blood Flow Metab*. 2019;39:939–958. DOI: 10.1177/0271678X19835552.

SUPPLEMENTAL MATERIAL

Data S1.

Supplemental Materials and Methods

The Institutional Animal Care and Use Committees of the Feinstein Institutes for Medical Research approved this study protocol. The data supporting the findings of this study are available from the corresponding authors upon reasonable request. The data that support the findings of this study are available from the corresponding author upon reasonable request.

Animal Preparation

We performed all instrumentation according to our previously described protocol(25). In brief, male Sprague-Dawley, male rats (450-550g, Charles River Laboratories, Wilmington, MA, USA) were anesthetized with 4% isoflurane (Isosthesia, Butler-Schein AHS, Dublin, OH, USA) and intubated with a 14-gauge plastic catheter (Surflo, Terumo Medical Corporation, Somerset, NJ, USA). The animals were mechanically ventilated (Ventilator Model 683, Harvard Apparatus, Holliston, MA, USA) at a minute ventilation (MV) volume of 180 mL/min and a respiratory rate (RR) of 45 breaths/min. In this study, we used one ventilation setting for all animals at all times and did not change the MV or RR over the experiments. Anesthesia was maintained with isoflurane 2%. The left femoral artery of each rat was cannulated (sterile polyethylene-50 catheter inserted for 20 mm) for continuous arterial pressure monitoring (MLT844, ADInstruments; Bridge Amplifier ML221, ADInstruments, Colorado Springs, CO, USA). A temperature probe (T-type thermocouple probes, ADInstruments Inc., CO, USA) was placed in the esophagus for continuous temperature monitoring. The core temperature was maintained at $36.5^{\circ}C \pm 1.0$ degree during the surgical procedure. The left femoral vein was cannulated with a polyethylene-50 catheter, which

was advanced into the inferior vena cava for drug infusion. At the end of the preparation, a blood sample (0.5 mL) was collected from the arterial catheter line, and a blood gas analysis (i-STAT; Heska, East Windsor, NJ, USA) was performed.

Experimental Protocol: Comparing Hyperoxia and Normoxia

Animals were randomly assigned into two groups at 10 minutes after CPR (Figure S1A). The post-resuscitation normoxic therapy group (n=15) included those who were successfully resuscitated from 10-minute asphyxia arrest and treated with inhaled 30% oxygen. The hyperoxia group (n=15) included those who were treated with inhaled 100% oxygen. After instrumentation, a neuromuscular blockade was achieved for all groups of animals through the slow intravenous administration of 2 mg/kg of vecuronium bromide (Hospira, Lake Forest, IL, USA). Asphyxia was induced by switching off the ventilator. CA occurred 3–4 minutes after asphyxia. After 10 minutes of untreated asphyxia, mechanical ventilation was restarted at an FIO_2 of 1.0. Manual CPR was delivered to all CA animals. The isoflurane inhalation was discontinued after the induction of asphyxia. Chest compressions were performed at a rate of 260-300 beat/minute. Immediately after CPR, a 20 μg/kg bolus of epinephrine was given to the animals through the venous catheter. Following the return of spontaneous circulation (ROSC), defined as a systolic blood pressure >60 mmHg, CPR was discontinued. If ROSC did not occur by 5 min of CPR, resuscitation was terminated. At ten minutes after CPR, the FIO_2 was switched back to 0.3 in the normoxic therapy group while it was kept at 1.0 in the hyperoxia group. Blood gas analysis was performed at 10, 20, 30, 45, 60, and 120 minutes after starting CPR. Mechanical ventilation was discontinued 120 minutes after CPR, survival was monitored up to 48 hours, and neurological deficit scores were obtained at 48 hours. Post-surgical care, including animal housing and observation, were provided

by the facility in a blinding manner.

Sham Experiments

Sham experiments with the rats at an FIO2 of 1.0 and FIO2 of 0.3 yielded tissue, tracheal secretion, and urine samples. Non-invasive metabolic measurements were performed at an FIO2 of 0.3 to achieve the normal numbers of our experimental setting.

VO2, VCO2, and RQ Measurements

Using the mechanical ventilation circuit, we evaluated the system-level metabolic alteration via VO2, VCO2, and RQ (VCO2 divided by VO2) of the rats. The details of these methods were described elsewhere by Shinozaki et al.(25). We added two major modifications to our previously reported methods in order to more accurately obtain VO2 at an FIO2 of 1.0: i) using a CO2 main-stream capnometer (Nihon Kohden Corp., Tokyo, Japan) to avoid sampling (suctioning) the gas from the ventilation system and ii) measuring the molecular ratio of inhalation to exhalation, which was an independent measurement from the gas concentration measurements. In addition, we used a photoluminescence-quenching sensor (FOXY AL300 Oxygen Sensor Probe, Ocean Optics, Dunedin, FL, USA) and a fluorometer (NEOFOX-GT, Ocean Optics, Dunedin, FL, USA) to measure the concentration of oxygen gas. Our circuit included a 10.5 mL mixing chamber on one side of the circuit, enabling each stroke of exhalation to be averaged in the chamber and throughout the circuit. We also used an inverted, water-sealed 500 mL cylinder filled with water to measure the volume of expired gas. Equations for evaluating the metabolism in this study are described as follows:

$$R = VI / VE \qquad\qquad (1)$$

$$VO2 = (R \times FIO2 - FEO2) \times VE \qquad (2)$$

$$VCO2 = FECO2 \times VE \qquad (3)$$

$$RQ = VCO2 / VO2, \qquad (4)$$

where R indicates the molecular ratio of inspiration and expiration; VI is the volume of inspiration; VE is the volume of expiration; FIO2 is the fraction of inspired oxygen; FEO2 is the fraction of expired oxygen; and FECO2 is the fraction of expired carbon dioxide. To correct the volume and gas concentrations, we measured the in-circuit gas pressure and temperature, relative humidity and temperature during exhalation, and ambient pressure and temperature around the ventilator circuit. The values were calculated and reported as standard temperature and pressure (STP).

Immunochemical Assays of Oxidative Stress Indicators HO-1 and HMGB-1 Levels

At 120 minutes after CA, eight rats were sacrificed from the sham-normoxia, sham-hyperoxia, CA-normoxia, and CA-hyperoxia groups. Immediately before sacrificing the animals, the anesthesia was reinduced, and the tissues were perfused. An 18-gauge needle was stuck into the left ventricle, and the perfusion was continued until the fluid draining from the left ventricle was clear, which required approximately 50 mL of 4°C extracellular solution. The blood was carefully removed from the collected tissue samples by washing with 4°C phosphate-buffered saline (PBS). The tissues were homogenized with protease inhibitors in PBS (at a tissue grams to PBS volume of 1:2) using a homogenizer and sonicater on ice. The homogenates were then centrifuged for 5 minutes at 5600×g twice, at which point we obtained the supernatant for the assays. The protein contents were determined using a bicinchoninic acid (BCA) protein kit (Pierce, Thermo Scientific, IL, USA), as per the manufacturer's instructions. The trachea secretion was sampled from the endotracheal catheter. The amount was weighed, and the catheter was washed with a dilution buffer

for the 8-hydroxydeoxyguanosine (8OHdG) measurement. The amount of dilution buffer was controlled to a dilution rate of 1:8. Urine samples were collected before the perfusion. The sample was centrifuged at 2,000×g, and the supernatants were obtained and diluted with a dilution buffer. The dilution rate of the urine sample was 1:8.

Carbonyl protein and 8OHdG levels were measured as an indicator of oxidative stress. HO-1 was used as an indicator of cytoprotective antioxidant enzymes and inflammation(27). HMGB-1 is an inflammatory alarmin that is released following nonprogrammed cell death but is not released by apoptotic cells(51). We measured HMGB-1 levels as an indicator of the activation of inflammatory pathway. The carbonyl protein (Enzo Life Sciences, Farmingdale, NY, USA) of the lung, brain, and kidney; 8OHdG (StressMarq Biosciences, Victoria, BC, Canada) of the urine and trachea secretion; HO-1 (Abcam plc, Cambridge, MA, USA) of the lung and brain; and HMGB-1 (Shino-test, Sagamihara, Kanagawa, Japan) of the lung and brain were measured by an enzyme-linked immunosorbent assay (ELISA) based on the commercial protocol. The sample absorbance was read on a 96-well plate reader at 540 nm. The numbers reported in this study are expressed relative to the protein content of the tissue samples.

Isolation of Brain and Kidney Mitochondria and Evaluation of Mitochondrial Respiratory Function

At 30 minutes after CA, eight animals were sacrificed from the sham-normoxia and CA-normoxia groups. All operations were performed at 4℃. The details of these isolation methods have been discussed elsewhere(20, 29). We homogenized the sample tissue using a Teflon/glass motor-driven homogenizer (model BDC2010, Glas Col LLC. Caframo, ON, CanadaTerre Haute, IN). A Sorvall

Legend X1R centrifuge (Thermo Scientific, Waltham, MA, USA) was also used. Low-speed centrifugation was conducted at 5600×g for 1 min, and high-speed centrifugation was conducted at 12000×g for 6 min. Mitochondrial yields were expressed as mg mitochondrial protein/g tissue. The mitochondrial isolation solution was mitochondrial isolation buffer (MESH)composed of 210 mM mannitol, 0.2 mM EGTA, 70 mM sucrose, and 10 mM Hepes at pH 7.3.

Kidney mitochondria isolation: After mincing and washing, the tissue was homogenized by 4 strokes. The homogenate was centrifuged at low-speed, and the supernatant was collected into a polycarbonate tube. This supernatant was then centrifuged at high speed. The supernatant was gently removed by pipets without disturbing the mitochondrial pellet. The pellet was finally resuspended in 20 mL of MESH without BSA and centrifuged at high speed. The mitochondria concentration was determined by the BCA assay, as mentioned above.

Brain mitochondria isolation: The minced brain tissue was homogenized by 8 strokes. The homogenate was centrifuged at low speed, and the supernatant was collected into a polycarbonate tube. The pellet was homogenized again and centrifuged using the same method described above, and the pooled supernatant was centrifuged at high speed. After high-speed centrifugation, the supernatant was removed gently until the synaptosome layer reached the top. The remaining loose pellet was suspended with 20 ml of 12.5% Percoll in MESH and centrifuged at high speed. The supernatant was gently removed by pipets without disturbing the mitochondrial pellet. The loose pellet was then homogenized by an additional 4 strokes of homogenizer in order to separate the mitochondria from the synaptosome contents, including the synaptic vesicles, postsynaptic membrane, and postsynaptic density. To that end, the pellet was resuspended in 20 mL of MESH buffer and centrifuged at high speed. Finally, the mitochondrial pellet was resuspended, and the mitochondria concentration was determined by the BCA assay.

Evaluation of isolated mitochondrial oxygen consumption: The oxygen consumption was measured using a Strathkelvin oxygen electrode (30℃). The mitochondria were assayed in an assay buffer containing 80 mM KCl, 50 mM MOPS, 1 mM EGTA, 5 mM KH_2PO_4, and 1 mg defatted BSA/mL at pH 7.4. ADP-dependent (state 3), ADP-limited (state 4), and DNP-dependent (uncoupled) respirations were measured in 150 µL of the mitochondrial suspension (0.5 mg/mL) using glutamate+malate as substrates. The rates of substrate oxidation were expressed as nano atoms oxygen consumed/minute/mg mitochondrial protein.

Comparing Mitochondrial H2O2 Generation in *ex vivo* Normoxic and Hyperoxic Conditions

H2O2 generation from the isolated mitochondria of the brain and kidney were used to determine mitochondrial ROS and we compared those from the sham-normoxia and CA-normoxia experimental groups. H2O2 levels were determined by an Amplex Red hydrogen peroxide/peroxidase assay kit (Invitrogen, Carlsbad, CA, USA) using the oxidation of the fluorogenic indicator Amplex Red in the presence of horseradish peroxidase, as instructed by the manufacturer. The fluorescence was recorded in a microplate reader Tecan Spark 10 M plate reader (Tecan Group Ltd., Männedorf, Switzerland) with 570 nm absorbance wavelengths. The standard curves were obtained by adding known amounts of H2O2 to an assay medium in the presence of the reactants (Amplex Red and horseradish peroxidase), which were linear up to 5 µM. The background fluorescence was measured in the absence of mitochondria and presented as fluorescence minus background (pmol/mg of protein/30 min). Following the protocols from previous studies(30), the mitochondria were incubated at 0.025 mg of protein/ml at 30°C. H2O2 production was initiated in the mitochondria using glutamate (10 mM) and malate (2.5 mM) as

substrates. With or without antimycin A (10 µM) as an addition to the incubation medium, we inhibited the activities of complex III, which allowed us to evaluate the isolated mitochondria.

Different O2 concentrations in the medium were achieved by mixing nitrogen- and air-saturated buffers. The mitochondrial oxygen tension was calculated at room temperature, and the atmospheric pressure (approximately 20°C and 760 Torr) and actual oxygen tension were measured by the photoluminescence-quenching sensor. We set up the medium at an O2 tension of 20–50 Torr in the normoxic condition and 150 Torr in the hyperoxic condition (Figure S5). Two different O2 tension settings were induced to isolate the mitochondria of the sham-normoxia and CA-normoxia animals, respectively.

Wet/Dry Weight Ratio of the Lung

At 120 minutes after CA, eight animals were sacrificed from the sham-normoxia, sham-hyperoxia, CA-normoxia, and CA-hyperoxia groups. The right lower lobe of each animal was weighed immediately after collection and then placed into a 60°C oven to dry. After three days, the tissue was weighed to determine the wet-to-dry lung weight as a lung wet/dry ratio (W/D). The right lower lobe was weighed immediately after collection and then placed into a 60°C oven to dry. After three days, the tissue was weighed to determine the lung W/D.

Immunofluorescence Staining of HO-1 and HMGB-1 and Histological Lung Injury Evaluation

At 120 minutes after CA, six animals were sacrificed from the sham-normoxia, sham-hyperoxia, CA-normoxia, and CA-hyperoxia groups. Tissues were transcardially perfused with 4°C extracellular fluid as described above and post-fixed overnight in 4% formalin in PBS for three

days at 4°C, then cryoprotected overnight in 30% sucrose in PBS at 4°C. The tissues were embedded in an M-1 Embedding Matrix™ (Thermo Scientific, Kalamazoo, MI, USA) and frozen in liquid nitrogen, cut serially (10 μm thickness) in a cryostat, and collected onto glass slides. After washing with tris-buffered saline (TBS), the sections were immersed in 10% normal goat serum (Sigma-Aldrich Co., St. Louis, MO, USA) in TBS containing 1% bovine serum albumin (BSA; Sigma-Aldrich Co., St. Louis, MO, USA) for 2 hours to block nonspecific binding.

For double immunostaining, the sections were incubated overnight with anti-HMGB-1 monoclonal antibody (Ab) (R&D systems, Inc., Minneapolis, MN, USA) or anti–advanced glycation end product (AGE) polyclonal Ab (Abcam plc, Cambridge, MA, USA) in combination with anti-HO-1 polyclonal Ab (Abcam plc, Cambridge, MA, USA) as the primary antibodies (Abs) at 4°C. Alexa 555–labeled anti-mouse IgG (Invitrogen Co., Branford, CT, USA) and Alexa 488–labeled anti-rabbit IgG (Invitrogen Co., Branford, CT, USA) were used as the secondary Abs. Sections were incubated with the secondary Ab at room temperature for 1 hour and mounted using a Vectorshield Hard Set mounting medium with 4',6-diamido-2-phenylindole (DAPI) (Vector Laboratories, Inc., Burlingame, CA, USA)(51). Stained sections were observed under an LSM 880 confocal imaging system (Carl Zeiss, Inc., Jena, Germany) and BZ-X800 all-in-one fluorescence microscope (Keyence, Elmwood Park, NJ, USA). We analyzed the data using the BZ-X800 analyzer software (Keyence, Elmwood Park, NJ, USA).

The lung sections were also stained with hematoxylin and eosin. After blinding the laboratory with respect to which group each rat belonged to, the histopathology was reviewed using a modified acute lung injury scoring system, as previously described elsewhere by Kawamura et al.(31) Four easily identifiable pathologic processes were

scored on a scale of 0–4, as previously described: i) alveolar congestion, ii) hemorrhage, iii) leukocyte infiltration or aggregation of neutrophils in airspace or the vessel wall, and iv) thickness of the alveolar wall. A total lung injury score was calculated as the sum of the four components.

Statistical Analysis

Data are shown as the means and SD for continuous variables and the counts and frequencies for categorical variables. An unpaired two-tailed Student t test or Mann-Whitney U test was used to compare two independent groups, as appropriate, for continuous variables. For post hoc comparisons, a one-way ANOVA or repeated ANOVA and Tukey test were used. Survival rates were estimated by the Kaplan-Meier method, and the Wilcoxon test was used to compare the groups. From our preliminary data, the survival rate at 48 hours after CA was expected as 80% in the normoxia group and 30% in the hyperoxia group. We anticipated that 12 animals per group were required for the survival study (α 0.05, power 0.8, two-sided). As the ROSC rate was estimated at 80%, we prepared 15 animals for each group. For measurements of oxidative stress indicator, based on our preliminary experiment, we generated a hypothesis of the difference of mean was 1.4-fold higher as compared to the control group and the standard deviation was 25% of the mean value (coefficient of variation = 25%); α 0.05, power 0.8, and two-sided analysis, were given to a power analysis of independent sample t-test. Two-tailed P values were calculated, and *p*<0.05 was considered statistically significant. SPSS 25.0 (IBM, Armonk, NY, USA), JMP 10.1 (SAS Institute, Cary, NC, USA), and GraphPad Prism 8 (GraphPad Software, San Diego, CA, USA) were used for statistical analyses.

Supplemental Results

The Post-Resuscitation Normoxic Therapy Improved Neurological Function and Survival after CA

No significant baseline differences were found between the groups. Fifteen rats for each group were assigned into the test group. There were two rats that did not achieve ROSC in the normoxic therapy group and one in the hyperoxia group. The normoxic therapy group had a higher survival rate (77%) at 48 hours after resuscitation compared to that (28%) of the hyperoxia group ($p<0.01$). The normoxic therapy group significantly improved across all survival rates and had lower neurological deficit scores (359±140 and 452±85, $p<0.05$) at 48 hours after CPR (Figure S1).

The Post-Resuscitation Normoxic Therapy Reduced System-Level Dissociations of Oxygen Metabolism

There were no significant differences in the values of PaO2 at 10 minutes between the CA-normoxia and CA-hyperoxia groups (302±76 and 361±71 Torr, respectively). In the normoxic therapy group, PaO2 was successfully maintained at 120±10 Torr during the initial 120 minutes after randomization. PaO2 levels in the hyperoxia group were higher than 350 Torr at all times.

There was no significant difference in the molecular ratio of inhalation to exhalation (R) between the CA-normoxia and CA-hyperoxia groups (1.0145±0.0078 and 1.0176±0.0052, respectively). In addition, the R of the sham animals showed no difference from that of the CA animals (1.0095±0.0055). At 120 minutes after CPR, the sham group had normal values of VO2, VCO2, and RQ (14.3±1.5 mL/kg/min at STP, 14.1±1.4 mL/kg/min at STP, and 0.99±0.12 respectively). At 120 minutes after CPR, the VO2 in the

CA-normoxia group had significantly lower numbers over time (17.8±3.1 mL/kg/min at STP) than it did in the CA-hyperoxia group (31.1±5.2 mL/kg/min at STP, $p<0.01$). There were no differences in VCO2 between the groups ($p=0.102$). At 120 minutes after CPR, the VCO2 was 14.3±2.3 mL/kg/min at STP for the CA-normoxia group and 17.9±3.3 mL/kg/min at STP for the CA-hyperoxia group. As a result, the RQ after CA was significantly higher in the CA-normoxia group (0.81±0.05) than it was in the CA-hyperoxia group (0.58±0.03, $p<0.01$), and the value for the normoxia group improved to the generally cited normal range of 0.7–1.0.

The Post-Resuscitation Normoxic Therapy Protected the Organs against Oxidative Stress

During hyperoxia, an increase in carbonyl protein of the brain occurred in the CA group (sham-normoxia and hyperoxia, 0.15±0.14 and 0.33±0.05 nmol/mg protein; CA-normoxia and hyperoxia, 0.32±0.23 and 0.93±0.13 nmol/mg protein, respectively). The carbonyl protein levels were [O2] dependent, and there was a trend in [O2] dependency in the sham group. However, hyperoxia-induced increases in carbonyl protein were more remarkable in the CA group ($p<0.01$).

In addition, during hyperoxia, an increase in carbonyl protein of the lung occurred in both the sham and CA groups (sham-normoxia and hyperoxia, 0.13±0.07 and 0.42±0.07 nmol/mg protein, $p<0.01$; CA-normoxia and hyperoxia, 0.28±0.15 and 1.00±0.14 nmol/mg protein, $p<0.01$, respectively). The carbonyl protein levels were [O2] dependent, and hyperoxia-induced increases in carbonyl protein were more remarkable in the CA group. Hyperoxia also increased the 8OHdG levels of the tracheal secretion in the CA group (sham-normoxia and hyperoxia, 3.2±1.5 and 5.6±0.5 ng/ml; CA-normoxia and hyperoxia, 7.6±1.2 and 20±6 ng/ml, respectively). A supply of 100% oxygen via the endotracheal tube did not affect the 8OHdG levels in the tracheal secretion samples from the sham animals. Consequently, [O2] dependency was only observed in the CA

animals ($p<0.01$). CA increased the 8OHdG levels beyond what was observed in the sham animals in both the normoxia and hyperoxia settings ($p<0.05$ and $p<0.01$, respectively).

During hyperoxia, an increase in carbonyl protein of the kidney also occurred in the CA group (sham-normoxia and hyperoxia, 0.08 ± 0.03 and 0.12 ± 0.04 nmol/mg protein; CA-normoxia and hyperoxia, 0.44 ± 0.18 and 0.99 ± 0.37 nmol/mg protein, respectively). The carbonyl protein levels were [O2] dependent, and there was a trend in [O2] dependency in the sham group. However, hyperoxia-induced increases in carbonyl protein were more remarkable in the CA group ($p<0.01$). Hyperoxia also increased the 8OHdG levels in the urine of the CA group (sham-normoxia and hyperoxia, 87 ± 63 and 39 ± 36 ng/ml; CA-normoxia and hyperoxia, 65 ± 34 and 168 ± 81 ng/ml, respectively). A supply of 100% oxygen did not affect the system level of 8OHdG in the sham animals tested by the urine samples, but [O2] dependency was observed in the CA animals ($p<0.01$). These results supported the idea that oxidative stress is [O2] dependent overall and can be seen in multiple organs. However, it was more remarkable after CA. Thus, post-resuscitation normoxic therapy significantly protected the animals against oxidative stress.

Cardiac Arrest Induces Mitochondrial Respiratory Dysfunction and the augmentation of O2-sensitive Mitochondrial H2O2 Generation

Oxidative phosphorylation: The state 3 respiration activity of the brain mitochondria in the CA-normoxia group (209 ± 26 nmol/min/mg) declined significantly compared to that of the sham-normoxia group (286 ± 50 nmol/min/mg, $p<0.01$). In contrast, the state 4 respiration activity of the brain mitochondria did not change significantly (sham and CA, 45 ± 13 and 44 ± 15 nmol/min/mg, respectively). As a result, the respiratory control

ratio (RCR) in the brain mitochondria showed a trend in derangement after CA (sham and CA, 6.6±1.4 and 5.1±1.6, $p=0.09$, respectively). The mitochondrial yield of the CA group was significantly lower than that of the sham group (sham and CA, 4.3±0.8 and 2.7±0.5, $p<0.01$, respectively). The state 3 respiration activity of the kidney mitochondria in the CA group (148±37 nmol/min/mg) declined significantly compared to that of the sham group (269±55 nmol/min/mg, $p<0.01$). In contrast, the state 4 respiration activity of the kidney mitochondria did not change significantly (sham and CA, 43±20 and 28±6.5 nmol/min/mg, respectively). There was a trend of declining RCR in the kidney mitochondria in the CA-normoxia group, but no statistical significance was identified (sham- and CA, 6.9±2.0 and 5.8±2.6, $p=0.32$, respectively). The mitochondrial yield of the CA group was significantly lower than that of the sham group (sham and CA, 22.6±1.3 and 18.4±1.7, $p<0.01$, respectively).

H2O2 generation in mitochondria: The *ex vivo* hyperoxic condition significantly accelerated the H2O2 generation of the brain mitochondria in both the sham and CA groups (sham-normoxic and hyperoxic condition, 66±13 and 84±29 pmol/mg protein, $p<0.01$; CA-normoxic and hyperoxic condition, 55±26 and 115±23 pmol/mg protein, $p<0.01$, respectively). Similarly, the *ex vivo* hyperoxic condition significantly accelerated the H2O2 generation of the kidney mitochondria in both the sham and CA groups (sham-normoxic and hyperoxic condition, 45±15 and 61±16 pmol/mg protein, $p<0.05$; CA-normoxic and hyperoxic condition, 44±14 and 89±39 pmol/mg protein, $p<0.05$, respectively).

The effect of the *ex vivo* hyperoxic condition on mitochondrial H2O2 generation was calculated for each animal, and the numbers were averaged and compared between the groups. The brain mitochondria generated approximately twice as much H2O2 in the hyperoxic condition (sham and CA, 125±20% and 267±203%, $p<0.05$, respectively). The kidney mitochondria also

showed a similar trend, but there was no statistical significance (sham and CA, 146±43%

and 268±250%, respectively). These results supported the augmentation of O2-sensitive

mitochondrial H2O2 generation after CA. This result might be attributed to the

mitochondrial dysfunction observed in the CA rat model.

In this experimental setting, hyperoxic condition did not affect the background

absorbance of Amplex Red reactions (Figure S6).

Hyperoxia Increased HO-1 Levels and Cardiac Arrest Increased both HO-1 and HMGB-1

Levels in the Brain

Immunohistochemical studies of the brain revealed O2-sensitive increase in HO-1 expression at

the subependymal cell layer and choroid plexus areas, and the hippocampus areas. The ratio of

HO-1 positive areas to DAPI positive areas showed that hyperoxia induced an increase in HO-1

expression at the hippocampus area in both the sham and CA groups (sham-normoxia and

hyperoxia, 0.04±0.02 and 0.13±0.02, $p<0.01$; CA-normoxia and hyperoxia, 0.09±0.02 and

0.14±0.02, $p<0.01$, respectively). Based on a comparison between the sham and CA animals at

normoxia ($p<0.01$), CA also seemed to induce HO-1 expression. A quantitative measure of HO-1

levels by ELISA showed a similar trend to the immunohistochemical studies (sham-normoxia and

hyperoxia, 0.39±0.03, 0.95±0.18 ng/mg protein; $p<0.01$; CA-normoxia and hyperoxia, 0.77±0.13

and 1.32±0.17 ng/mg protein, $p<0.01$, respectively). HO-1 levels in the CA group were higher

than in the sham group at normoxia ($p<0.01$). These results strongly support the idea that there is

an increase in HO-1 expression in the brain after CA and that its expression is O2 sensitive.

Immunohistochemical studies of the brain also revealed a post-CA increase in

HMGB-1 at the subependymal cell layer and choroid plexus areas, and the hippocampus

areas. The ratio of HMGB-1 positive areas to DAPI positive areas showed that CA increased the HMGB-1 levels at the hippocampus (sham-normoxia and hyperoxia, 0.03 ± 0.02 and 0.06 ± 0.03; CA-normoxia and hyperoxia, 0.14 ± 0.04 and 0.32 ± 0.08, respectively). A quantitative measure of HMGB-1 levels by ELISA showed a similar trend to the immunohistochemical studies (sham-normoxia and hyperoxia, 38.1 ± 5.5 and 42.8 ± 3.1 ng/mg protein; CA-normoxia and hyperoxia, 125 ± 4 and 133 ± 2 ng/mg protein, respectively). There might be a correlation between O2-sensitive increase and HMGB-1 levels, but it was only observed post-CA. CA increased the HMGB-1 levels in the brain. However, in contrast to what occurred with HO-1, the O2-sensitive augmentation was not clearly observed in the sham animals.

Cardiac Arrest Was Associated with Hyperoxic Lung Injury

The lung W/D ratio revealed that hyperoxia increased lung edema after CA (sham-normoxia and hyperoxia, 4.4 ± 0.6 and 4.7 ± 0.2; CA-normoxia and hyperoxia, 4.6 ± 0.4 and 5.6 ± 0.5, $p<0.01$, respectively). The lung injury score histologically exhibited a similar trend: that hyperoxia increased the degree of lung injury at 120 minutes after CPR (sham-normoxia and hyperoxia, 2.7 ± 2.3 and 2.3 ± 1.0; CA- normoxia and hyperoxia, 4.3 ± 2.9 and 14 ± 2, $p<0.01$, respectively). These results supported the idea that hyperoxia induces lung injury and that it is more remarkable post-CA (Figure S2).

Hyperoxia Increased HO-1 Levels and Cardiac Arrest Increased both HO-1 and HMGB-1 Levels in the Lung

Immunohistochemical studies of the lung revealed the O2-sensitive increase in HO-1 expression in the sham animals. However, there was an increase and suppression of HO-1 by the hyperoxia

after CA. The ratio of HO-1 positive areas to DAPI positive areas showed that hyperoxia increased the HO-1 in the sham group but not in the CA group (sham-normoxia and hyperoxia, 0.06±0.06 and 0.78±0.11, $p<0.01$; CA-normoxia and hyperoxia, 0.77±0.15 and 0.57±0.07, respectively). A quantitative measure of HO-1 levels by ELISA showed a similar trend to those of the immunohistochemical studies (sham-normoxia and hyperoxia, 5.2±0.5 and 12.4±1.0 ng/mg protein, $p<0.01$; CA-normoxia and hyperoxia, 10.5±1.4 and 6.5±0.5 ng/mg protein, $p<0.01$, respectively).

Immunohistochemical studies also revealed an increase in HMGB-1 in the lung after CA. The result of the ratio of HMGB-1 positive areas to DAPI positive areas showed that CA but not hyperoxia increased the HMGB-1 levels in the lung (sham-normoxia and hyperoxia, 0.02±0.04 and 0.06±0.02; CA-normoxia and hyperoxia, 0.33±0.10 and 0.68±0.16, $p<0.01$, respectively). Moreover, immunohistochemical studies of the lung indicated an increase in AGE expression, especially in the CA-hyperoxia group. A quantitative measure of HMGB-1 levels by ELISA showed a similar trend to that of the immunohistochemical studies (sham-normoxia and hyperoxia, 199±46, 221±36 ng/mg protein; CA-normoxia and hyperoxia, 471±51 and 716±49 ng/mg protein, $p<0.01$, respectively). There might be a correlation between the O2-sensitive increase and HMGB-1 levels, but it was only observed post-CA. These results suggest that HO-1 expression in the lung is O2-sensitive, but there might be a paradoxical suppression of HO-1 expression post-CA during hyperoxia. CA increased the HMGB-1 levels in the lung. Given the immunohistochemical finding of AGE expression in conjunction with an increase in HMGB-1, our results indicated that the inflammatory HMGB-1 pathway might be activated post-CA.

Supplemental Discussion

The mitochondrial ROS generation during hyperoxia might be one of the causal factors upregulating the pathways of oxidants.

Mitochondrial O2 tension at a temperature of 37°C has been estimated to be in the order of several Torr(52). However, the most recent *in vivo* study suggested that it was as high as 50 and 100 Torr(53). Mitochondrial ROS generation is generally measured in an air-saturated medium at a temperature ranging from 20 to 37°C(30), in which the amount of oxygen dissolved in the medium is at a setting equivalent to the partial oxygen pressure between 150 and 178 Torr at atmospheric pressure. Therefore, an air-saturated medium in most experimental settings creates an unnatural hyperoxic condition for mitochondria, which is considered 2–3 folds or even 30–50 folds higher than that for physiological mitochondrial O2 tension.

Danilov(17) tested astrocyte cell death from ischemia/reperfusion injury at an oxygen tension of 50 and 150 Torr (i.e., 7% and 21% oxygen), respectively, and showed a protective effect from the lower (physiologically normal) oxygen tension. We tested whether the [O2] dependency of mitochondrial ROS generation increased after CA using an oxygen tension of 50 and 150 Torr, respectively. The brain and kidney mitochondria isolated from the animals suffering from CA exhibited approximately two times more H2O2 generation than those of the sham animals. We were in general agreement that the ROS generation by electron leakage occurred at the blocked respiratory complex I and complex III in the METC(30) and observed consistent results in our CA rodent models(20, 21). Therefore, it was inferred that post-resuscitation hyperoxia may exacerbate mitochondrial ROS generation due to increased electron leakage from a dysfunctional METC attributed to post-CA ischemic/reperfusion injury.

Post-CA syndrome is a pathophysiological condition of systemic ischemia/reperfusion

injury affecting the multiple organ sytem(48). In particular, lung-brain coupling is a new pathophysiological concept introduced by Mai and Halterman(54). Since the lung plays an important role as a site of inflammation and neutrophil priming, the lung can process the systematic inflammation post-CA. Given our pathological findings, it can be inferred that the increased amount of ROS might contribute to post-CA hyperoxic lung injury.

Figure S1. Post-Resuscitation Normoxic Therapy Improved Neurological Function and Survival in a rat CPR model.

A

B

C
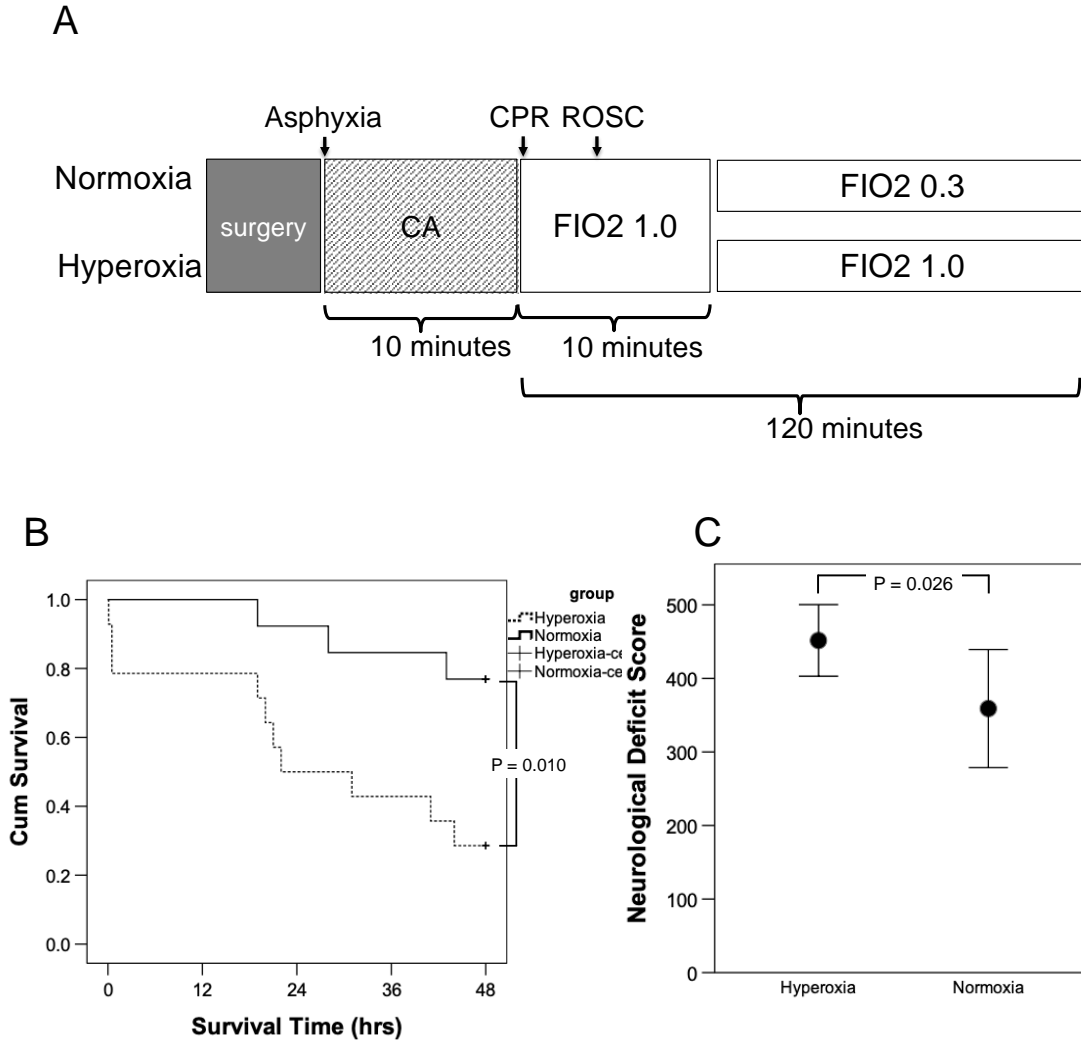
A, Experimental protocol. Animals were assigned into two groups at 10 minutes after CPR. The post-resuscitation normoxic therapy group (n=15) included those who were successfully resuscitated from 10-minute asphyxia arrest and treated with inhaled 30% oxygen. The hyperoxia group (n=15) included those who were treated with inhaled 100% oxygen. B, Kaplan-Meier survival curve of CA animals: the hyperoxia group (n=14) and normoxia group (n=13) were included. Animals that did not achieve ROSC (n=1, n=2, respectively) were excluded. *P* value was calculated by Wilcoxon test. C, Neurological deficit score at 48 hours after CA. The hyperoxia group (n=14) and normoxia group (n=13) were included. Numbers were presented as mean and SD. *P* value was calculated by Mann-Whitney U test. CA indicates cardiac arrest; CPR, cardiopulmonary resuscitation; ROSC, return of spontaneous circulation; FIO2, fraction of inspired oxygen.

Figure S2. Mitochondrial oxygen tension during an incubation time in the medium at an ex vivo normoxic condition.
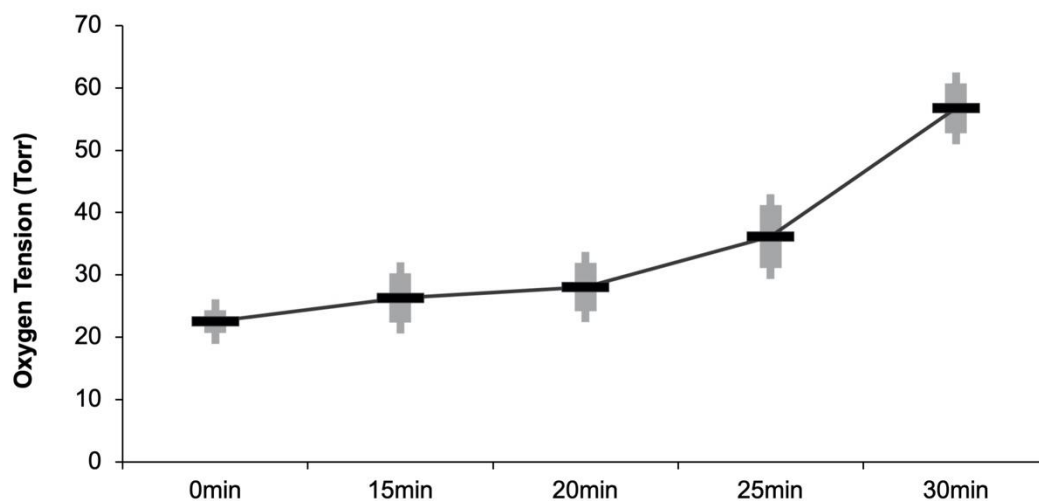

The substrates, reaction buffer, and mitochondria were added in the medium for this preliminary experiment. Photoluminescence-quenching sensor was used to measure the oxygen tension in the medium at room temperature and atmospheric pressure. Both temperature and atmospheric pressure was monitored during the experiment and oxygen tension was calculated from these numbers.

Figure S3. The Back-Ground H2O2 Levels of Amplex Red reactions in our Experimental Setting.
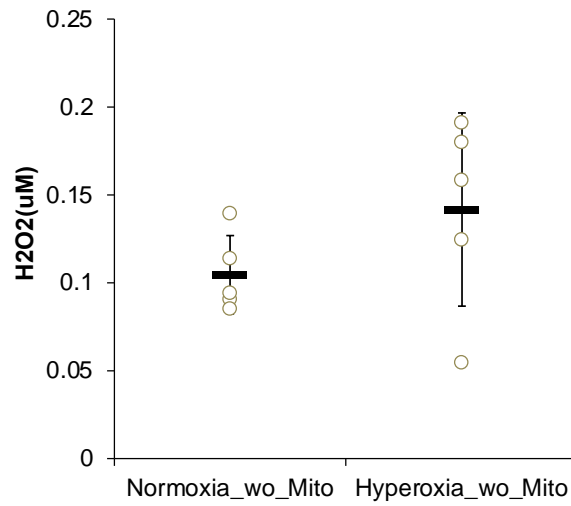

The test samples were prepared without mitochondria but all contents including the substrates and reaction buffers were the same. *Ex vivo* Hyperoxic condition did not affect the back-ground measurements and therefore we verified that our experimental condition was not [O2] dependent.

**Figure S4. Hyperoxia Induced Lung Injury after CA.**
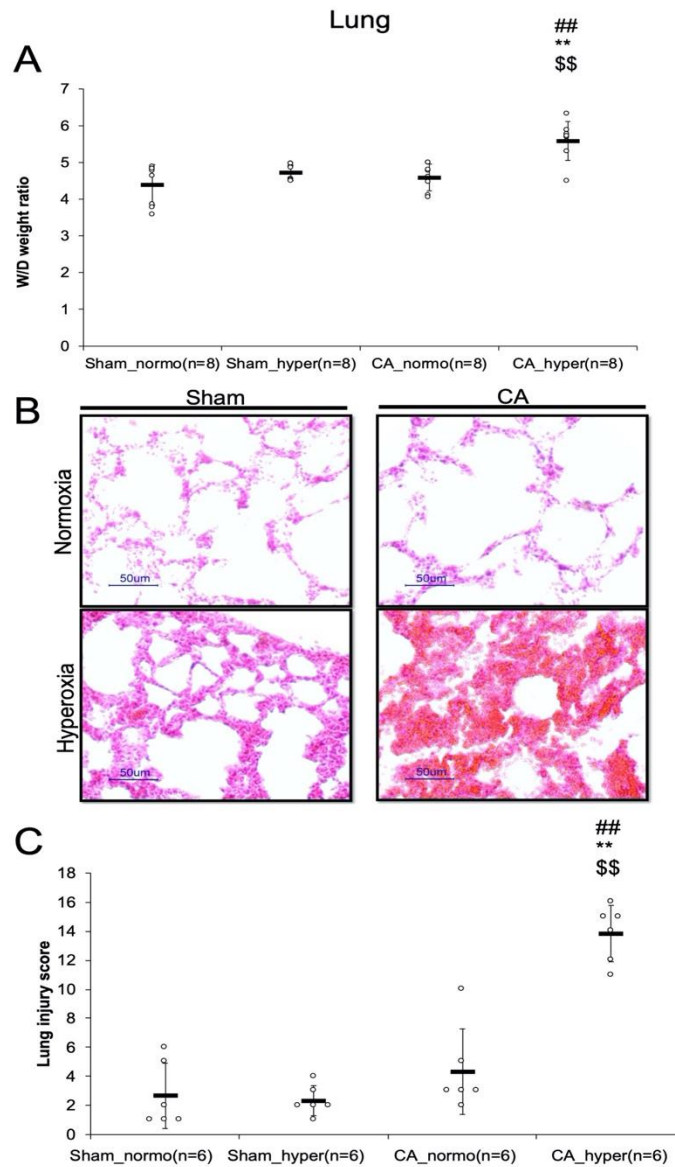
A, Wet/Dry weight ratio of the lung. The lung W/D ratio revealed that hyperoxia increased lung edema after CA. B, Lung histology. The blue bars represent a scale of 50 μm. C, Lung injury score compared among the 4 groups. The lung injury score histologically exhibited that hyperoxia increased the degree of lung injury at 120 minutes after CPR. ## $p<0.01$ vs Sham normoxia. ** $p<0.01$ vs Sham hyperoxia. $$ $p<0.01$ vs CA normoxia.

Figure S5. Post-cardiac arrest hemodynamic status.
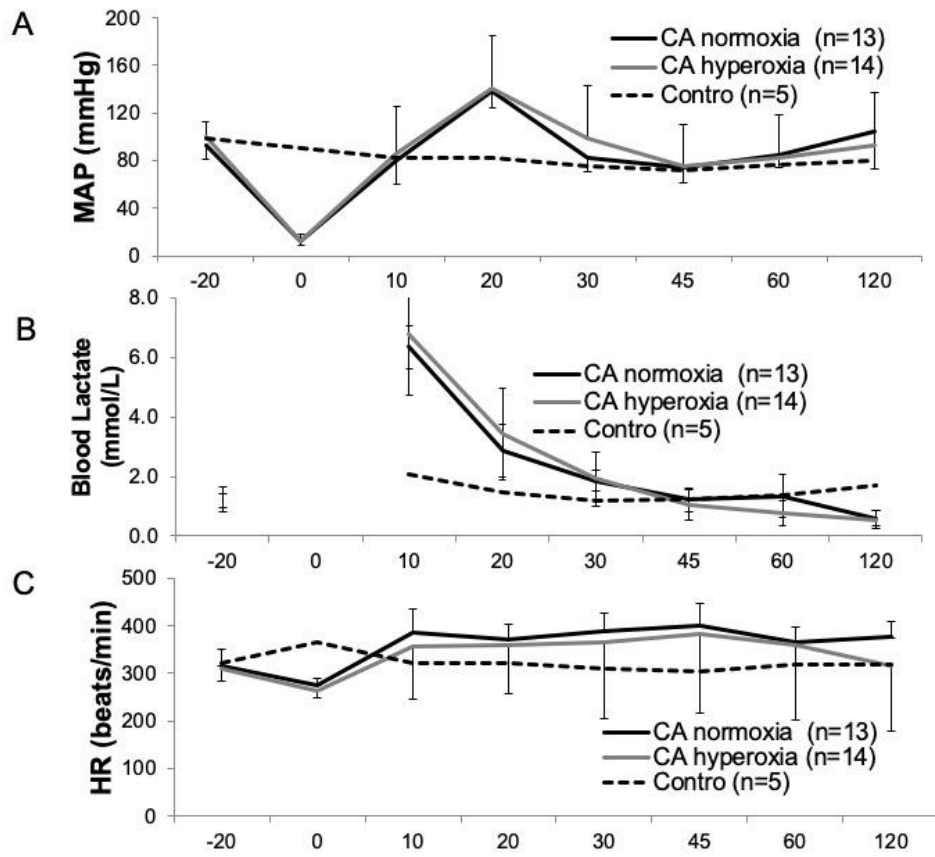
A, mean arterial pressure; B, blood lactate level; C, heart rate, among the three groups over a 120-minute of observational period.

Figure S6. Post-resuscitation normoxic therapy did not affect carbonyl protein levels in the heart.
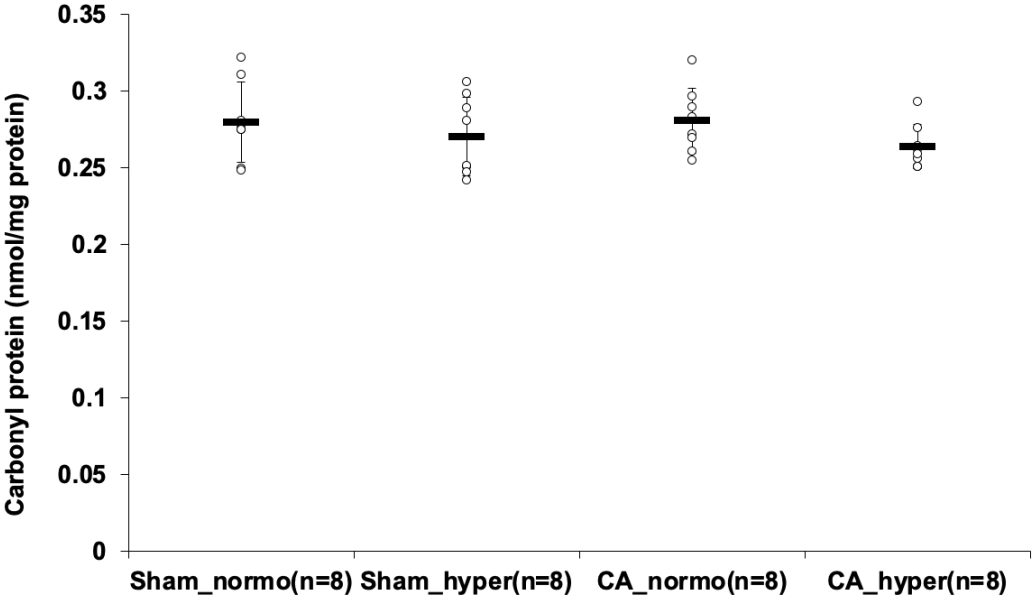
We did not observe any augmentations in carbonyl protein levels among the groups.